

Article

Methodological Approach (In Situ and Laboratory) for the Characterisation of Late Prehistoric Rock Paintings—*Penedo Gordo* (NW Spain)

Jose Santiago Pozo-Antonio ^{1,*} , Beatriz Comendador Rey ², Lara Alves Bacelar ³ and Pablo Barreiro ⁴

¹ CINTECX, GEESMin Group, Dpto. de Enxeñaría dos Recursos Naturais e Medio Ambiente, Escola de Enxeñaría de Minas e Enerxía, University of de Vigo, 36310 Vigo, Spain

² Grupo GEAAT, Dpto. de Historia, Arte e Xeografía, Facultade de Historia, Campus das Lagoas, University of Vigo, 32004 Ourense, Spain; beacomendador@uvigo.es

³ Centre for Studies in Archaeology, Arts and Heritage Sciences (FCT/CEAACP), University of Coimbra, 3004-531 Coimbra, Portugal; larabacelar@sapo.pt

⁴ CINTECX, Novos Materiais Group, Dpto. de Física Aplicada, Escola de Enxeñaría Industrial, University of Vigo, 36310 Vigo, Spain; pbarreiro@uvigo.es

* Correspondence: ipozo@uvigo.es; Tel.: +34-986814077

Abstract: This paper draws on the study of the prehistoric art site of *Penedo Gordo* (NW Spain) resulting from a collaborative interdisciplinary research. One of its primary goals was to design and put into practice a multi-analytical protocol for characterising prehistoric rock paintings, combining in situ and laboratory analytical techniques. Thus, following the archaeological assessment of the site, the panels exhibiting red paintings were analysed by colour spectrophotometry and portable Raman spectroscopy. Analytical techniques were applied to a collection of samples exhumed from the excavation that simultaneously took place on site. These included three red accretions on different substrates (compact soil, white quartzite and grey quartzite) and stone fragments representative of the outcrop's petrographic variability, aiming to determine their mineralogical composition, texture and study the stone-paint boundaries. Moreover, colouring materials exhumed from the excavation and collected in the immediate surroundings of the rock outcrop were analysed in order to scrutinise the provenience rock art's raw materials. Laboratory analysis consisted of stereomicroscopy, X-ray diffraction, Fourier transform infrared spectroscopy and scanning electron microscopy. One of the major outcomes was the discovery of a drop of red pigment preserved in an archaeological layer associated with Late Neolithic/Copper Age material remains.

Keywords: prehistoric rock painting; pigment; archaeology; schematic art; cultural heritage; hematite; goethite



Citation: Pozo-Antonio, J.S.; Comendador Rey, B.; Alves Bacelar, L.; Barreiro, P. Methodological Approach (In Situ and Laboratory) for the Characterisation of Late Prehistoric Rock Paintings—*Penedo Gordo* (NW Spain). *Minerals* **2021**, *11*, 551. <https://doi.org/10.3390/min11060551>

Academic Editors:
Domenico Miriello, Raffaella De Luca and Michele Secco

Received: 12 April 2021

Accepted: 20 May 2021

Published: 22 May 2021

Publisher's Note: MDPI stays neutral with regard to jurisdictional claims in published maps and institutional affiliations.



Copyright: © 2021 by the authors. Licensee MDPI, Basel, Switzerland. This article is an open access article distributed under the terms and conditions of the Creative Commons Attribution (CC BY) license (<https://creativecommons.org/licenses/by/4.0/>).

1. Introduction

Penedo Gordo is a Late Prehistoric rock art site that was recently discovered in south-eastern Galicia (Spain). The investigation carried out in 2018 followed a novel research protocol for the study of Schematic Art rock paintings in northwest Iberia, based on a multi-disciplinary approach that included rock art recording, excavation, edaphic and sedimentary studies, radiocarbon dating, geophysical surveys as well as historical and anthropological inquiries [1]. Regarding the analysis of the decorated surfaces, the aim was to combine the recording of both the paintings and backdrop with an assessment of their state of conservation, identification of biological colonies (particularly lichens) as well as their physical, chemical and mineralogical characterisation [2].

As known, the recipes of prehistoric paintings most frequently include inorganic substances, mainly red-orange and black pigments that might have been mixed with organic binders of vegetable or animal origin [3–6]. In Iberia, black pigments were mainly produced from charcoal or soot and red pigments were composed of hematite (Fe₂O₃) or red

ochre [6]. The latter is a natural earth in which iron oxides and hydroxides are mixed with clay but also with minerals such as quartz (SiO_2), dolomite ($\text{CaMg}(\text{CO}_3)_2$), hydromagnesite ($\text{Mg}_5(\text{CO}_3)_4(\text{OH})_2 \cdot 4\text{H}_2\text{O}$), calcite (CaCO_3), aragonite (CaCO_3), gypsum ($\text{CaSO}_4 \cdot 2\text{H}_2\text{O}$), muscovite ($\text{KAl}_2(\text{AlSi}_3\text{O}_{10})(\text{OH})_2$), feldspar ($(\text{K}, \text{Na}, \text{Ca}, \text{Ba}, \text{NH}_4)(\text{Si}, \text{Al})_4\text{O}_8$), etc. [7,8]. When hematite is dominant, a red colour is exposed, while in iron oxides and hydroxides such as goethite (FeOOH) or sienna, the colouration tends to a yellowish tone [8,9]. In ochres, although the Fe content is lower than the clay content even at concentrations below 1%, the colour obtained is red [8,9].

It is worth pointing out that the analytical techniques applied to determine the chemistry and mineralogy of the different constituents, such as petrographic microscopy, scanning electron microscopy, Raman spectroscopy, Fourier transform infrared spectroscopy, X ray diffraction, etc., require the extraction of microsamples. However, physical properties such as colour or reflectance are not habitually measured, even though they may be useful to determine physical changes and possible material losses. A combined characterisation of the chemical, mineralogical and physical properties allows us to address fundamental issues such as the identification of the different deterioration forms affecting the structure of both the paintings and the backdrop, alteration agents such as water circulation or biological colonisation, etc. Ultimately, the results obtained may be applied to support the establishment of preventive conservation measures aiming to delay the degradation of rock art panels. Despite the quantity and quality of the work developed on this subject in recent years [4,6–8,10–17], a comprehensive protocol to guide the characterisation of rock paintings, considering its chemical, mineralogical and physical properties, has not yet been established.

Moreover, considering the deontological code of cultural heritage conservation [18], any initiative that involves acting on a rock art site needs to reduce the impact of sampling on decorated panels. This makes it difficult to characterise the entire collection of motifs at a particular rock art site. Therefore, non- or micro-destructive in situ analytical techniques are preferred. Although Raman spectroscopy or Fourier transform infrared spectroscopy have shown their portable modalities, micro-samples of paintings are still commonly brought to laboratory for analysis [3,6,7,12,13,15–17]. Only a few scientific works in this field of study were found to have applied Raman spectroscopy in situ [14,19]. For instance, the combination of in situ and laboratory Raman spectroscopy in the study of El Reno Paleolithic cave art allowed a complete chemical and mineralogical characterisation of the paintings [14]. Thus, more research applying portable systems is required. Moreover, the aesthetical analyses of painted surfaces using colour spectrophotometry could be useful even for monitoring, since colorimetric variations may indicate chemical and mineralogical alterations. This is another portable technique that is yet to be regularly used for the characterisation of prehistoric rock paintings.

This article describes the application of an analytical protocol to the Late Prehistoric rock paintings at Penedo Gordo [20], in connection with the progress of the archaeological work on site. This investigation offered a rare occasion to relate a number of samples collected from the stratigraphy of a trench excavated immediately below one of the decorated walls with in situ and laboratory analysis. The rock art assemblage, distributed across five panels in opposing areas of the rock outcrop, was recorded by using different techniques of digital photography including D-Stretch, colour spectrophotometry and Raman spectroscopy. Two samples of rock and one of soil exhumed from excavation showing red-coloured material were the object of laboratory analysis in order to determine the mineralogical, chemical and textural properties of the coloured layer using stereomicroscopy, X-ray diffraction, Fourier transform infrared spectroscopy and scanning electron microscopy. Moreover, possible colorant materials found in excavation and stone fragments representative of the different rock facies found in the outcrop were also analysed from textural, chemical and mineralogical perspectives.

Thus, the evidence gathered from rock art recording and excavation raised a number of questions that we expected to be tackled by physical and chemical analysis:

- Could they bring additional data to inform us about the sequence of rock art production on site?
- To what extent could these analyses help us distinguish between red patches of pigment and natural mineral intrusions present in decorated panels?
- Does the red coat found on stone fragments exhumed in excavation correspond to natural mineral intrusions or actual paint? Could the samples bearing red mineral intrusions have been a local source of raw material for prehistoric paintings?

2. Materials and Methods

2.1. The Rock Art Site: Penedo Gordo (Vilardevós, Ourense, NW Spain)

Penedo Gordo was the second painted rock shelter to be identified in Galicia, a region best known for the presence of Atlantic Art open-air carvings in the western regions [20]. It is located in the hinterland, near the hamlet of Feilas, in the parish of Fumaces and Trepa, municipality of Vilardevós (Ourense) (Figure 1A,B).

The site sits halfway upslope of a hill range flanked by the valley of river Tamega to the southwest and the heights of Serra Seca to the northwest. It stands as an isolated and conspicuous rock measuring ca. 20 m × 30 m × 20 m sitting in an area geologically dominated by quartzite from the Silurian-Devonian period [21] (Figure 1C,D). The outcrop shows three variations of different colour: a white rock with an orange-coloured layer, a dark grey rock and a black stone with a dark-brown colouration rock.

The presence of rock paintings on the site was first noticed by B. Rúa and J.L. Lozano in October 2017. Soon after, B. Comendador (co-author of this article) visited the site and informed governmental authorities of its scientific relevance. In the following year, the Directorate General of Heritage invited the University of Vigo to elaborate a research proposal to carry out the recording of the rock art and a small-scale excavation.

Field research conducted in 2018 allowed the discovery of paintings on five different panels on both the northern and the western areas of the outcrop (Figures 1C and 2). The techno-morphological features of the motifs confirmed the preliminary attribution of this assemblage to the Schematic Art tradition. This is a Late Prehistoric rock art tradition shared across the European Mediterranean biogeographical region whose northwesternmost limits are now located in the Galician heartland (Spain) [20]. It is typically painted on the walls of shallow rock shelters, cliff walls or small caves and tends to occur at liminal places in the landscape. Its repertoire is dominated by the presence of the human figure reduced to its minimal details but also displays geometric motifs such as dots, bars and grids. In Iberia, this tradition is believed to have its origins in the late 6th/5th millennium BC [20].

As stated, the recording of the rock art was complemented with the excavation of two trenches located below the rock outcrop's surfaces containing rock paintings. On the northern area, excavation revealed stratified deposits dated to the beginning of the 4th millennium BC and to the mid. 3rd millennium BC [2]. It was therefore possible to attest the presence of human activities immediately below the rock art panels whose origin can be potentially dated to a period between the regional Early/Middle Neolithic and the Late Neolithic/Copper Age, yet not ruling out an earlier chronology.

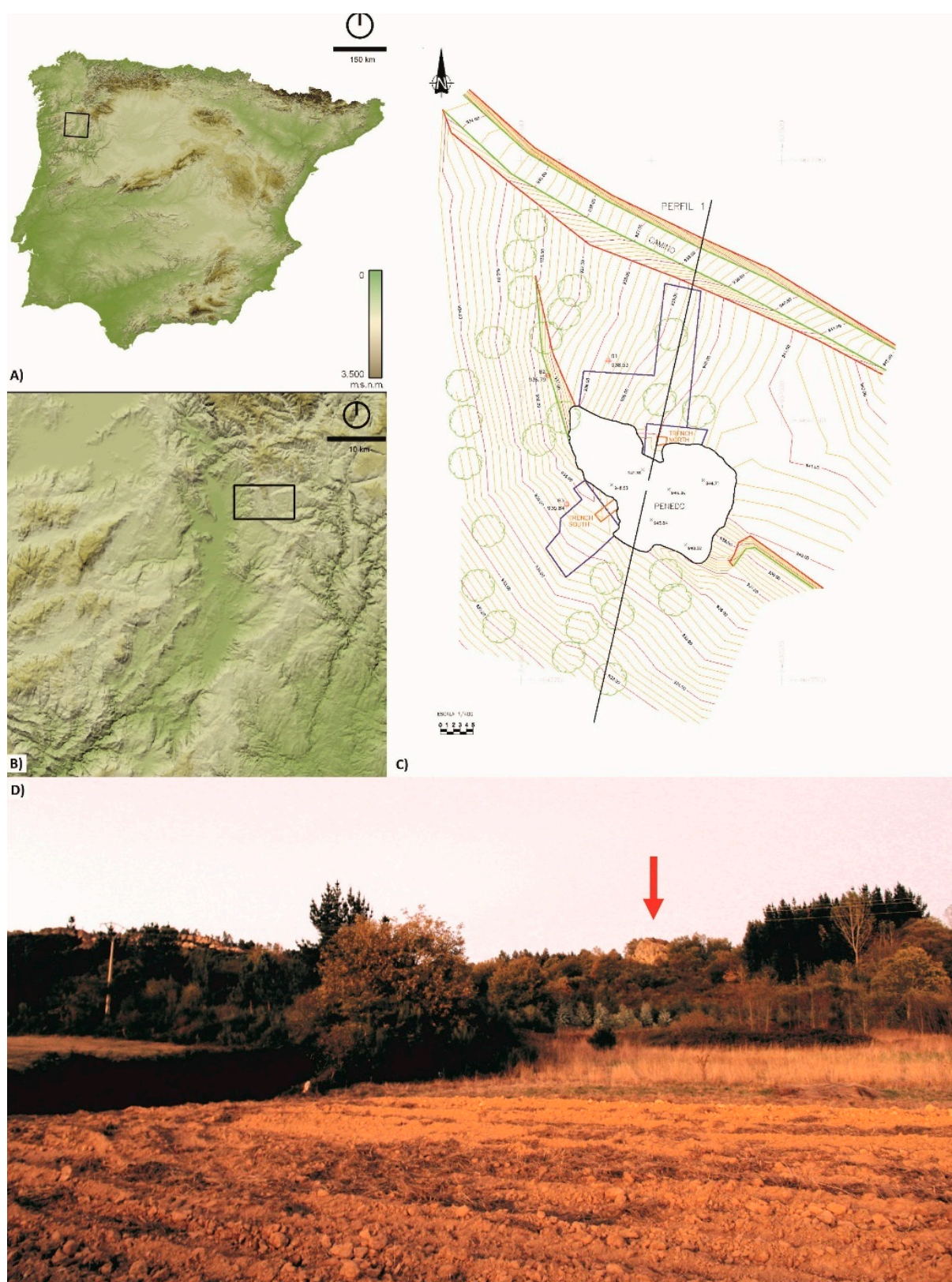


Figure 1. (A,B): Location of Penedo Gordo (Vilardevós, Ourense) in NW Spain. (C): Contour survey of the site with the rock outcrop in the centre, indicating the two areas where motifs were located and the sitting of the two trenches. (D): A view of the outcrop from lower parts of the south-eastern slope.

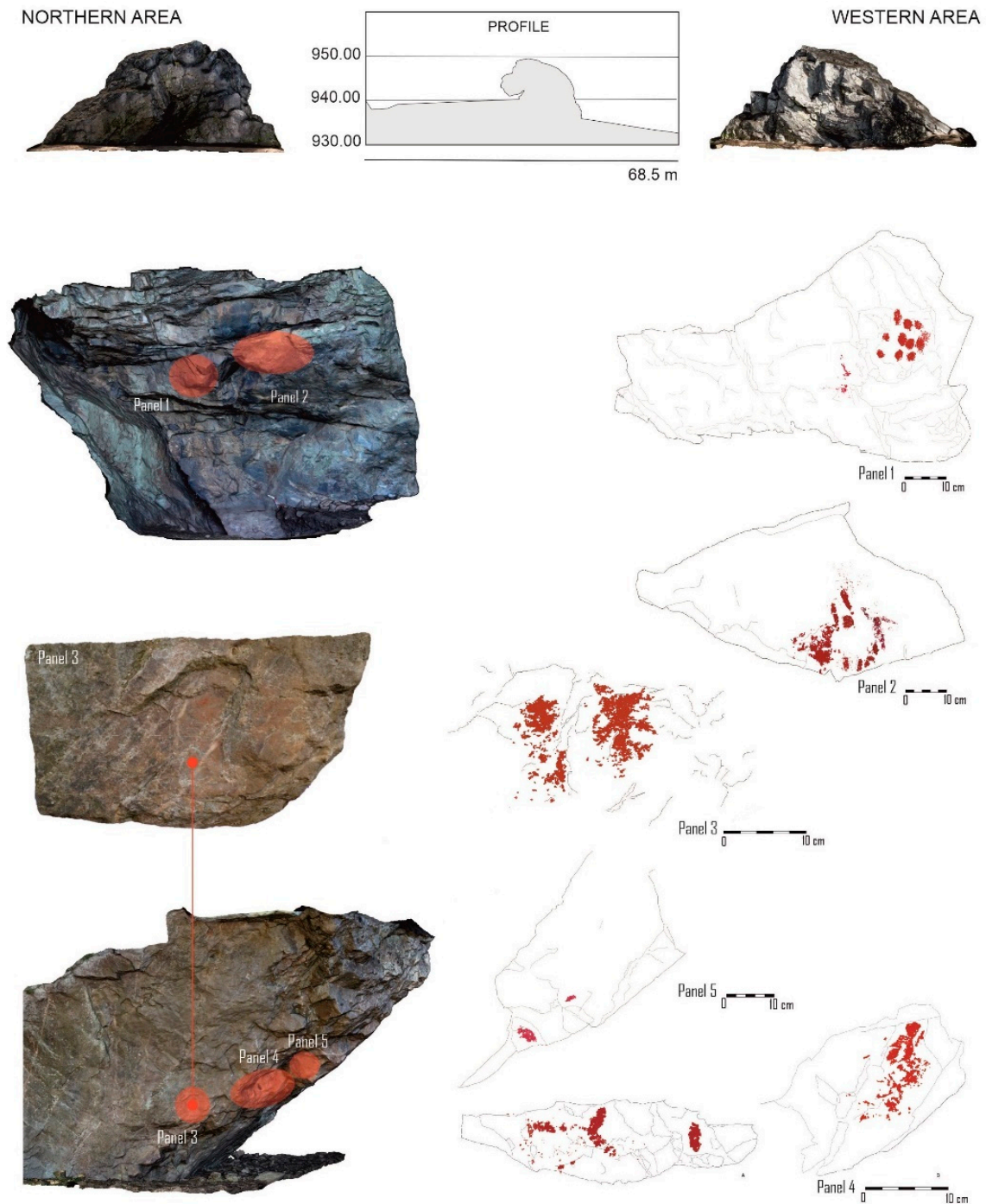


Figure 2. The two areas of Penedo Gordo displaying Schematic Art paintings, showing the range of motifs found in each panel.

2.2. Analytical Protocol

2.2.1. In Situ Characterisation

The first stage of the analytical protocol consisted of the rock art recording combining direct and vector tracing of images subjected to digital photographic enhancement. Digital photographs were taken with a Canon 5D Mark II. In order to identify the number and morphological features of the painted motifs, the surfaces were imaged using DStretch (<https://www.dstretch.com> (accessed on January 2018)), a plugin for ImageJ developed by John Harman. Once the motifs (M) were catalogued, both their colour and the colour

of the stones in the outcrop of all five panels were measured using spectrophotometry. A Sampling point (Sp) on each motif was identified. The measurements were obtained with a portable spectrophotometer (Konica Minolta CM-700d, Tokyo, Japan) equipped with CM-S100w (SpectraMagic™ NX, Tokyo, Japan) software. The working conditions of the device were as follows: area view (MAV) of 8 mm, CIE standard daylight Illuminant D65 and observer 10°, with Specular Component Excluded (SCE) mode. The colour was measured in the CIELAB space [22]. Therefore, the colour parameters measured were: L*, lightness, which varies from 0 (absolute black) to 100 (absolute white); a*, associated with changes in redness–greenness (positive a* is red and negative a* is green); and b*, associated with changes in yellowness–blueness (positive b* is yellow and negative b* is blue). For each Sp, twenty measurements were made.

As a spectroscopic technique, Raman spectroscopy was used to detect the molecular composition of the pigments and the stones. Raman spectroscopy was applied in the same Sp where colour measurements were performed. Excitation at 785 nm was provided by a continuous wave diode laser, coupled to an optical head. Individual areas of measurement were controlled with a light-emitting diode and a high-resolution colour camera. The scattered radiation was collected through the objective lens, passed through an edge filter that cut off Rayleigh scattering, and focused into an optical fibre that was fed into a compact spectrograph, equipped with a concave grating, providing spectral coverage in the 120–3395 cm⁻¹ range at a spectral resolution of about 10–15 cm⁻¹. The detector, a Synapse™ CCD (1024 × 256 pixels), was Peltier-cooled and featured high sensitivity with low dark counts. During the analysis, the power delivered by the laser beam on the sample surface was adjusted to 30 mW, exposure time was 10 s and spectra corresponded to an average of 2–5 consecutive scans on the same point. Three Raman spectra were taken from each Sp.

2.2.2. In Laboratory Characterisation

Soon after the in situ characterisation was carried out, the excavation of the northern trench located below panels 3 and 4 revealed the above mentioned samples with red-coloured surfaces (Table 1):

- A fragment of a grey quartzite showing a red-coloured deposit covered by a dark soil patina (hereinafter PG, Table 1).
- A compact piece of soil containing a thick layer of a red substance (hereinafter PE, Figure 3 and Table 1).
- A fragment of white quartzite with a red-coloured deposit, and as PG also covered by a dark earth patina (hereinafter PW, Table 1).

Table 1. Samples collected in Penedo Gordo, with a digital photograph for each sample, the identifications (ID) used in this article and the inventory of the excavation, the area A—(N: North or W: West), the UE and the XYZ coordinates.

ID (Inventory ID)	A	Description	UE	X Coord.	Y Coord.	Z Coord.
PG (PG18SNp003)						
	N	Fragment of a grey quartzite showing a red-coloured deposit covered by a dark soil patina	Ue205	637,502.114	4,647,736.408	939.84

Table 1. Cont.

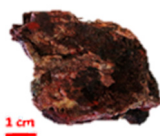
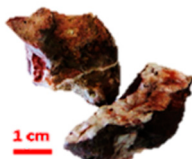
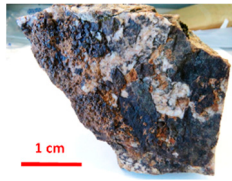
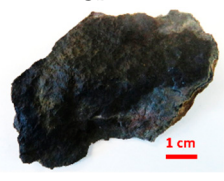
ID (Inventory ID)	A	Description	UE	X Coord.	Y Coord.	Z Coord.
PE (PG18SNp007)						
	N	Compact piece of soil with a thick layer of a red substance	Ue208/Ue209	637,501.69	4,647,737.16	939.88
PW (PG18p130)						
	N	Fragment of a white quartzite with a red deposit	Ue218	637,501.31	4,647,736.85	939.78
PGMT1 (PG18SOp016)						
	W	Possible colorant material collected in the western trench	Ue105	-	-	-
PGMT2 (PG18SNp062)						
	N	Possible colorant material collected in the northern trench	Ue214	637,502.02	4,647,736.46	939.73
PGMT3 (PG18SNp068)						
	N	Possible colorant material collected in the northern trench	Ue209/Ue213	637,501.44	4,647,736.90	939.81
PGMT4 (PG18SNp085)						
	N	Possible colorant material collected in the northern trench	Ue213	637,501.24	4,647,737.32	939.84
SW						
	W	A white quartzite with a dark patina on the surface		Collected near the W area.		

Table 1. Cont.

ID (Inventory ID)	A	Description	UE	X Coord.	Y Coord.	Z Coord.
SBB 	W	A quartzite with a dark-brown colouration				Collected near the W area.
SB 	W	A dark grey quartzite				Collected near the W area.

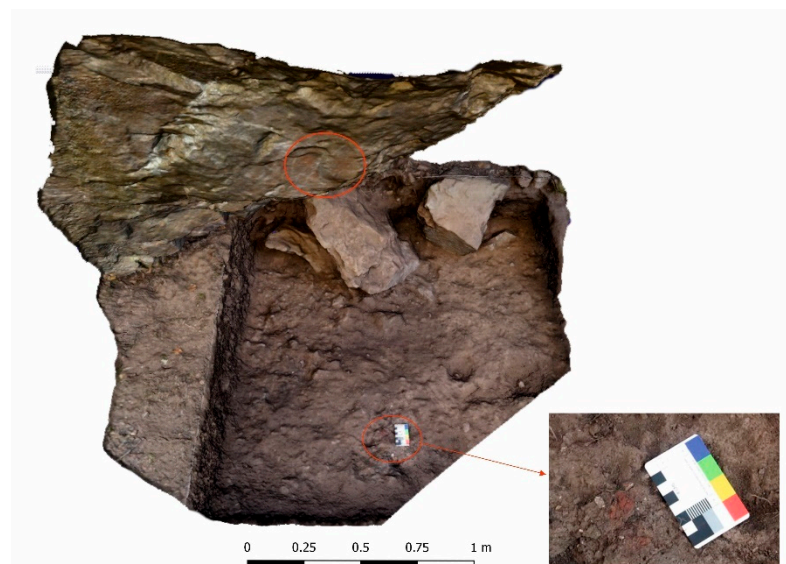


Figure 3. Location of the compact piece of soil with a thick layer of a red substance (PE). This sample was collected in the northern trench excavated under panels 3 and 4.

Moreover, possible colorant materials were also found during the excavation of both trenches (Table 1):

- A laminar red stone (PGMT1) was collected in the western trench.
- A granular red stone (PGMT2) was collected in the northern trench.
- Two white stones with red-coloured deposits (PGMT3 and PGMT4) were collected in the northern trench.

Macroscopically, these samples show similar tones of red.

In order to characterise the different quartzite facies of the painting's backdrop, three fragments with different colourations representative of those commonly found in the outcrop were collected from its immediate vicinities in the western area (Table 1):

- A white quartzite with a dark patina on the surface (hereinafter SW).
- A quartzite with a dark-brown colouration (hereinafter SBB).
- A dark grey quartzite (hereinafter SB).

The samples collected were investigated in the laboratory using the following protocol:

Firstly, all samples were examined by stereomicroscopy (SMZ800 NIKON[®], Tokyo, Japan) in order to physically characterise the red-coloured deposits in the samples, stone fragments and possible colorant materials.

The mineralogical composition of all the samples was determined by X-ray diffraction (XRD, Siemens D5000, München, Germany), applying the random powder method. For the red-coloured surface samples found in excavation, the red deposit was scraped off the surface using a punch. For the remaining stones and possible colorant materials, small fragments were obtained using a chisel and a geological hammer. The black layer detected on the SW sample was also extracted with a punch. Samples were ground in a mechanical ball mill. Analyses were performed using Cu-K α radiation, Ni filter, 45 kV voltage, and 40 mA intensity. The exploration range was 3° to 60° 2 θ and the goniometer speed was 0.05° 2 θ s⁻¹. The abundance of each mineral phase (semi-quantitative estimation) was calculated using highest intensity diffraction peaks and intensity ratios (reflection power) established from artificial mixtures of standard minerals [23].

The molecular composition of red deposits scraped from the coloured surface samples (PG, PE and PW) was detected by Fourier transform infrared spectroscopy (FTIR) (Thermo Nicolet[®] 6700, Waltham, MA, USA) in attenuated total reflectance (ATR) mode using an FTIR Thermo Nicolet[®] Continuum. The FTIR spectra were recorded in absorbance mode in the 4000–400 cm⁻¹ region, with 4 cm⁻¹ resolutions.

All the samples were embedded with an epoxy resin (EpoThin 2 Epoxy Resin and EpoThin 2 Epoxy Hardener). Once hard, a transversal cut was made to obtain specimens measuring 2 cm × 2 cm × 1 cm. These cross-sections were visualised by stereomicroscopy (SMZ800 NIKON[®], Tokyo, Japan). Later, the cross-sections were coated using carbon, and they were visualised using scanning electron microscopy (SEM) with energy dispersive X-ray (EDX) spectroscopy (FEI Quanta 200) in backscattered (BSE) and secondary (SE) electrons modes. Optimum conditions of observation were obtained for an accelerating potential of 20 kV, a working distance of 10–11 mm and a specimen current of 60 mA.

3. Results

3.1. *In Situ Analysis of the Rock Art: Paintings and Backdrop*

Based on digital photographs, enhanced photographic images and vector drawings, the rock art catalogue was produced prior to data collection by spectrophotometry and Raman spectroscopy. Figure 4 shows digital photographs of the different coloured rock facies found in the outcrop (SW: Figure 4A; SBB: Figure 4B; SB: Figure 4C) and digital photographs, enhanced photographic images and vector drawings of the panels and the motifs (M). The location of the Sampling point (Sp) is shown where colour spectrophotometry and Raman spectroscopy were applied.

On panel 1, paintings were found on two different sectors (Figure 4D,E,G,H). On the right, an assemblage of eleven dots painted with the fingertips was detected (Figure 4E,F) and on the left, a surface below exhibits three inconspicuous and weathered painted lines (Figure 4F,H). Panel 2, found 50 cm to the right of the former, is equally an open-air surface, yet even more exposed to the environment (Figure 4I–K). This explains the extremely weathered conditions in which the paintings were found. The panel shows, on the left-hand side, dots and bars typical of the Schematic Art tradition and on the right, remains of paintings forming a group of lines barely visible to the naked eye and that were only able to be recorded by enhanced digital photography. Regarding the northern area, panel 3 is equally exposed to the environment and exhibits, on the right, a human figure with a triangular-shaped head and, on the left, patches of pigment that may have belonged to a second motif now decayed (Figure 4L–O). These figures showed a colouration slightly more orange than the rest of the motifs. Panel 4 corresponds to a white quartz intrusion in the quartzite outcrop and sits in a more sheltered area (Figure 4P–T). This seems to have contributed to a better preservation of the pigment for it shows the brightest and most solid colour of the whole assemblage. Nevertheless, these motifs were difficult to classify due to weathering. On the left-hand side, two vertical bars were recognised, one of them attached

to two others set at an angle and, on the right sector of the panel, there is a degraded coat of paint superimposed on an indeterminate figure (Figure 4T). Panel 5 shows a small oval-shaped form likely to have been produced by a fingertip and a shapeless patch of pigment (Figure 4U–W).

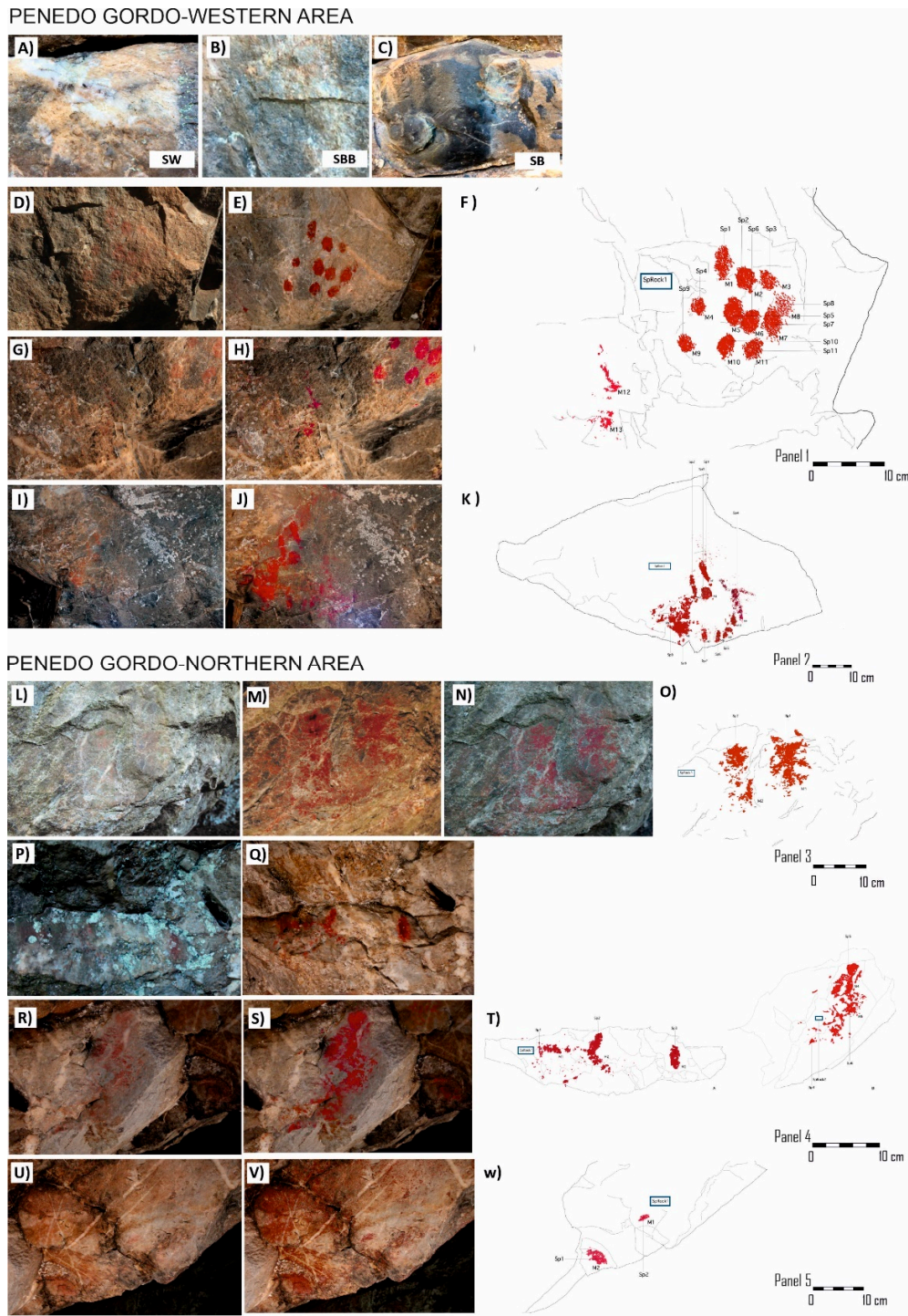


Figure 4. (A–C): Quartzite facies in the outcrop with different colouration (SW: white quartzite, SBB: quartzite with a dark brown colouration, SB: dark grey quartzite). (D–V): Penedo Gordo’s motifs (M) and Sampling points (Sp) identified in panel 1 (D–H), panel 2 (J,K), panel 3 (L–N), panel 4 (P–T) and panel 5 (U–W).

Figure 5 and Table 2 shows the colour data obtained; L^* , a^* and b^* measurements for each Sp, but also, the measurements for the most representative colours detected on the natural surface of the outcrop (Figure 5A,G,M): white (SW), brown-black (SBB) and dark grey (SB). A lighter colour (higher L^*) for the SW sample was identified compared to those for the SBB and SB samples (Figure 5A), confirming its white colouration. For the SW and SBB samples, they had positive a^* (Figure 5G) and b^* (Figure 5M) values, showing a slight orange colouration of the main white and black colouration, respectively. However, negative values of these parameters were detected by SB due to its dark colour.

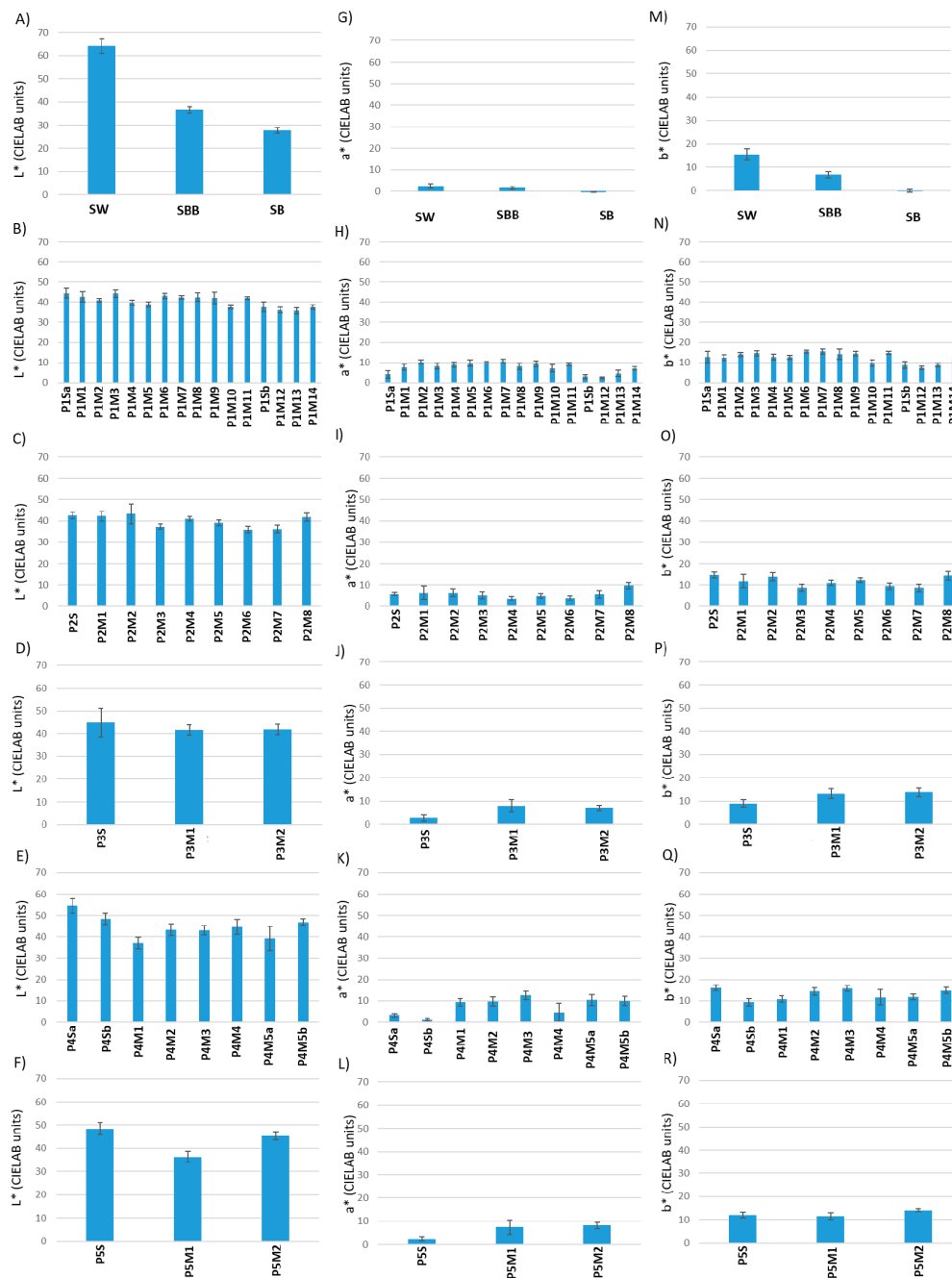


Figure 5. Colorimetric parameters L^* (A–F), a^* (G–L) and b^* (P–R) of the stones (A,G,M) and Sp detected in the northern (P1: (B,H,N); P2: (C,I,O)) and western panels (P3: (D,J,P), P4: (E,K,Q); P5: (F,L,R)) of Penedo Gordo.

Table 2. Colorimetric parameters L*, a* and b* with their standard deviations (\pm std) of the stones (SW, SBB and SB) and Sp detected in the panels of the northern and western areas of Penedo Gordo. In addition, the parameters for the stones lacking paintings identified in each panel (SW, SBB and SB) are shown.

Stones and Panels	Sample	L*	\pm std	a*	\pm std	b*	\pm std
Stones	SW	64.04	3.02	2.53	1.05	15.54	2.44
	SBB	36.68	1.36	1.57	0.65	6.78	1.28
	SB	27.74	1.17	−0.40	0.10	−0.16	0.61
Panel 1	P1SpR1	44.51	2.36	4.13	1.88	12.71	2.75
	P1Sp1	42.65	2.52	7.71	1.49	12.40	1.42
	P1Sp2	41.03	0.86	10.24	0.93	14.01	0.92
	P1Sp3	44.27	1.76	8.25	1.39	14.64	1.22
	P1Sp4	39.69	1.16	8.97	1.26	12.65	1.41
	P1Sp5	38.85	1.38	9.73	1.48	12.61	1.07
	P1Sp6	43.18	1.33	10.00	0.49	15.50	0.75
	P1Sp7	42.48	0.91	10.58	1.01	15.44	1.25
	P1Sp8	42.52	2.05	8.04	1.59	14.22	2.65
	P1Sp9	42.10	2.91	9.29	1.53	14.47	1.13
	P1Sp10	37.53	0.83	7.16	1.83	9.76	1.59
	P1Sp11	42.01	0.77	9.15	0.66	14.85	0.82
	P1SpR2	37.67	2.49	2.91	0.92	8.83	1.68
	P1Sp12	36.13	1.42	2.38	0.44	7.28	0.85
P1Sp13	35.72	1.46	4.55	1.55	8.64	0.83	
P1Sp14	37.51	1.17	6.99	0.92	11.20	0.98	
Panel 2	P2SpR1	42.54	1.70	5.84	0.57	14.54	1.39
	P2Sp1	42.19	2.34	6.33	3.13	11.76	3.01
	P2Sp2	43.39	4.71	6.34	1.81	13.81	1.85
	P2Sp3	37.32	1.27	5.15	1.69	8.74	1.59
	P2Sp4	40.88	1.04	3.64	0.98	10.87	1.19
	P2Sp5	39.07	1.44	4.93	0.96	12.27	1.12
	P2Sp6	35.89	1.48	3.88	1.03	9.41	1.53
	P2Sp7	36.15	1.74	5.62	1.83	8.57	1.68
P2Sp8	41.70	1.93	9.64	1.52	14.21	2.07	
Panel 3	P3SpR1	44.76	6.31	2.63	1.28	8.99	1.60
	P3Sp1	41.61	2.32	7.94	2.81	13.19	2.12
	P3Sp2	41.87	2.28	7.01	1.24	13.78	1.90
Panel 4	P4SpR1	54.51	3.34	3.11	0.98	16.16	1.26
	P4SpR2	48.39	2.74	1.15	0.56	9.31	1.78
	P4Sp1	37.16	2.65	9.34	1.75	10.88	1.56
	P4Sp2	43.38	2.61	9.72	2.16	14.45	1.73
	P4Sp3	43.15	2.15	12.54	2.06	15.91	1.46
	P4Sp4	44.66	3.58	4.53	4.35	11.66	3.62
	P4Sp5	39.25	5.71	10.38	2.53	11.83	1.42
P4Sp6	46.95	1.53	10.09	2.15	14.85	1.48	
Panel 5	P5SpR1	48.50	2.65	2.38	0.83	12.02	1.20
	P5Sp1	36.39	2.25	7.44	3.07	11.52	1.53
	P5Sp2	45.37	1.73	8.20	1.32	14.15	0.68

Moreover, for each panel, the natural colour of the rock lacking painting is also shown in Figure 5 in order to compare with that of the motifs; the colour of the stone is identified by an R (from rock) added to the panel's ID (P1SpR1 and P1SpR2 for each sector of panel 1, P2SpR1, P3SpR1, P4SpR1 and P4SpR2, because the rock on panel 4 showed two different colourations and P5SpR1). Comparing the colour parameters measured (L^* , a^* and b^*) of the Sp with those of the rocks lacking paintings, although nuances were not very intense, it was possible to distinguish different trends:

- For the Sp from panels 1 (Figure 5B,H,N) and 5 (Figure 5F,L,R), the parameter a^* was the one with more statistically significant differences comparatively to the value recorded on the original rock (P1SpR1, P1SpR2 and P5SpR1). The a^* increase confirms the presence of a red painted layer on the surface.
- For the motifs from panels 2 (Figure 5C,I,O) and 4 (Figure 5E,K,Q), L^* was the parameter showing more statistically significant differences when compared with its values for the unpainted rocks (P2SpR1, P4SpR1); this fact reveals a darkening of the surface. Although L^* changes were negligible in most of the cases considering the standard deviations, the coloured surfaces tended to show L^* decreases (darkening).
- For the motifs from panel 3 (Figure 5D,J,P), the parameter b^* showed more statistically significant differences regarding the value of the rock (P3SpR1); b^* increases are associated with a more orange tone, which was also detected under the naked eye.

Figure 6 shows the Raman spectra of the motifs and rocks from each panel. In the Raman spectra of the SBB and the SB samples (Figure 6A), strong peaks were identified that could be assigned to Si-O-Si at 206 cm^{-1} and 466 cm^{-1} [24–27] due to the presence of quartz. Moreover, in the SB and also in the black layer detected on the white sample (SW-black layer in Figure 6A), weak peaks at 1360 and 1580 cm^{-1} were found; they are attributable to amorphous carbon [6]. It is important to highlight that these particular Raman peaks assigned to amorphous carbon can be modified due to the different conditions during the measurement [28]. Raman peaks in the spectral region 1000 – 1600 cm^{-1} are attributed to the presence of charcoal or soot likely derived from the combustion of vegetable materials [3,6,16]. Therefore, these black layers on the white rock can be attributed to fire ignitions that took place in this more sheltered area over time [6,13]. Moreover, the high fluorescence detected in the Raman spectra of the black layer suggested its organic composition. The orange patches detected on the rock surfaces (orange stains in Figure 6A) were analysed by Raman spectroscopy in order to distinguish between natural features and the painted motifs, because macroscopically, they may be mistaken. The Raman spectra of the orange stains detected peaks at 226 cm^{-1} , 293 cm^{-1} , 412 cm^{-1} and 612 cm^{-1} (this latter almost inappreciable), suggesting the presence of hematite (Fe_2O_3) [29]. However, this Raman spectrum did not show fluorescence revealing, therefore, the lack of organic compounds in them. Therefore, using Raman spectroscopy, it was possible to distinguish between the natural orange stains in this stone and the red paintings.

Considering the Raman spectra from the Sp, in addition to the peak at 206 and 466 cm^{-1} revealing the presence of silicate minerals, a highly intense peak of the hematite at 293 cm^{-1} was detected in most of them; this peak of greater or lower intensity was found in the spectra of all the Sp from panel 1 (Figure 6B), panel 4 (Figure 6E) and panel 5 (Figure 6F) and those of Sp2, Sp3, Sp5 to Sp8 from panel 2 (Figure 6C). Goethite, whose main Raman peaks are 301 cm^{-1} and 386 cm^{-1} , was identified mainly through the latter, on panel 2 (Sp6 and Sp7 with higher intensity and Sp8 and Sp4 with lower intensity) and panel 3.

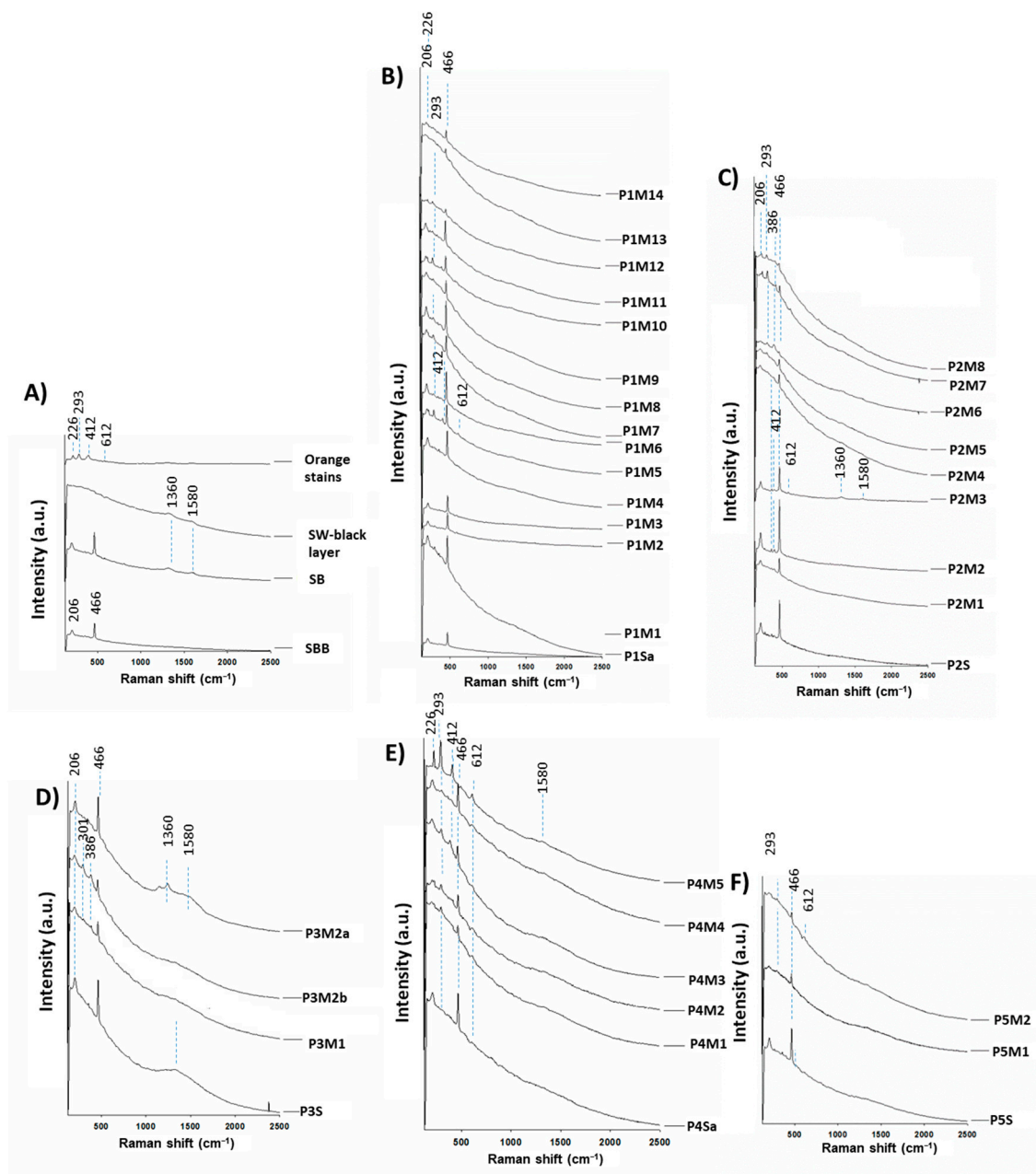


Figure 6. Raman spectra of the rock surface (A) and Sp (B–F) detected on the panels of the northern (Panel 1: B, Panel 2: C) and western (Panel 3: (D); Panel 4: (E); Panel 5: (F)) areas of Penedo Gordo.

Moreover, it is also important to highlight the presence of peaks at 1360 and 1580 cm⁻¹ for the Raman spectra of the Sp from panels 2 (Sp3), 3 (Sp2) and 4 (Sp5), assigned to amorphous carbon [6]. On panel 3, for Sp2, two Raman spectra are depicted in Figure 6D, because of the heterogeneity in its composition: one spectrum suggesting the presence of amorphous carbon in the darkest part (P3Sp2a) of the motif and one spectrum suggesting the presence of goethite (P3Sp2b). P3SpR1 showed a Raman spectrum with a broad peak in the range 1200–1600 cm⁻¹ (Figure 6D), which is assigned to amorphous carbon [6], showing higher intensity than that detected in the SB sample (Figure 6A). It is worth reiterating that the presence of amorphous carbon can be related to recent wildfires or hearths whose remains are still visible nearby. Moreover, making a comparison between the Raman spectra of the backdrop, P3SpR1 was the unpainted surface revealing both the highest fluorescence and highest presence of organic matter.

3.2. Laboratory Characterisation

Stereomicroscopy allowed the characterisation of the appearance and extension of the samples collected (Figure 7). Regarding the coloured surface samples found in excavation, it was possible to find an intense red colouration on the surfaces mainly on PE (Figure 7A). The coloured layer showed a variable thickness.

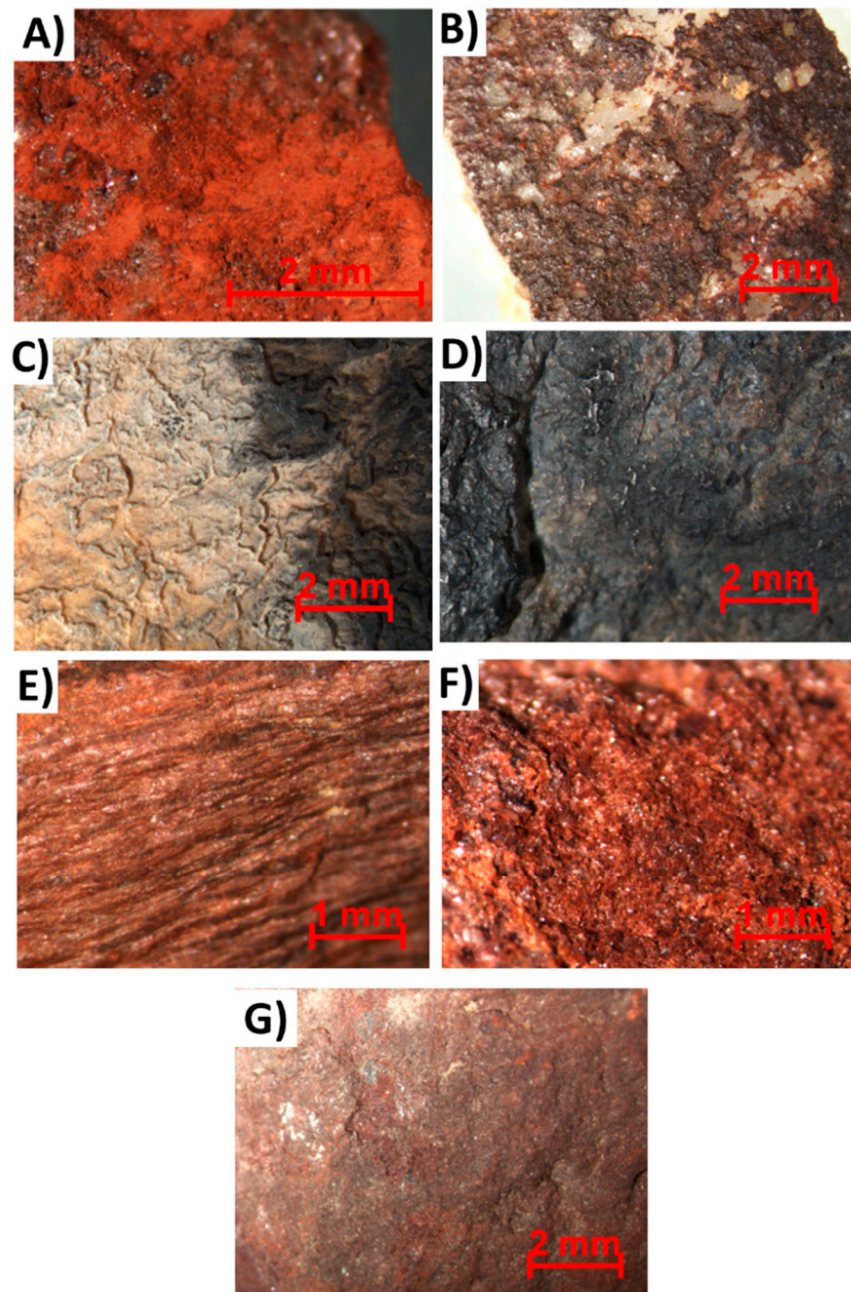


Figure 7. Micrographs taken with stereomicroscopy of the samples collected; red-coloured drop on the soil (A) stones (B–D), and colorant material (E–G). (A): PE. (B): SW. (C): SBB. (D): SB. (E): PGMT1. (F): PGMT2. (G): PGMT3.

The stones collected, despite belonging to the rock outcrop, showed different colourations and textures. SW was covered almost completely by a discontinuous black-brown-coloured layer (Figure 7B) with variable thickness. Under this layer, it was possible to identify an orange-coloured layer. SBB (which was attested to show colourations from brown to black) displayed the characteristic opal-A speleothems (Figure 7C), specifically identified

as flowstone [30–32]. SB was the darkest one (Figure 7D) and showed a black colouration with brown iridescence. Moreover, incipient opal speleothems were also detected.

Considering the possible colorant materials exhumed from the excavation, the samples collected exhibited different textures. PGMT1 showed laminated structures (Figure 7E), PGMT2 was composed of a granulated structure, while PGMT3 (Figure 7F) and PGMT4 were composed of a granular structure but more compact than PGMT2 (Figure 7G).

The mineralogical composition detected by XRD (Table 3) confirmed that the red deposits scraped were mainly composed of quartz (SiO_2) and hematite ($\alpha\text{-Fe}_2\text{O}_3$). PE in addition showed calcite (CaCO_3) and jarosite ($\text{KFe}_3(\text{SO}_4)_2(\text{OH})_6$) and PW, muscovite ($\text{KAl}_2\text{Si}_3\text{AlO}_{10}(\text{OH})_2$) and rectorite ($(\text{Na, Ca})\text{Al}_4((\text{Si, Al})_8\text{O}_{20})(\text{OH})_4\cdot 2\text{H}_2\text{O}$). PE was the red-coloured surface sample showing the highest amount of hematite. Regarding the natural stones collected around the outcrop (SW, SBB and SB), they were composed mainly of quartz. SB also showed lepidocrocite ($\gamma\text{-FeOOH}$), anhydrite (CaSO_4) and jarosite. In SW, in addition to quartz, goethite ($\alpha\text{-FeOOH}$) and anhydrite were identified. Note that none of the stones from the outcrop showed hematite in the composition, confirming Raman spectroscopy results. The dark layer on the white sample (SW-black layer) showed quartz and mainly, goethite. Regarding the colorant materials collected from the excavation, the four samples were composed of quartz and hematite. PGMT1 also contains plagioclase ($\text{NaAlSi}_3\text{O}_8$), potassium feldspar (KAlSi_3O_8), anhydrite and butlerite ($\text{Fe}(\text{OH})\text{SO}_4\cdot 2\text{H}_2\text{O}$). PGMT2 also showed muscovite and PGMT3 revealed, in addition to quartz and hematite, traces of anhydrite. PGMT1 and PGMT2 include a higher hematite content than the other two colorant materials PGMT3 and PGMT4.

Table 3. Mineralogical composition by XRD (random powder). Q: Quartz (SiO_2); P: Plagioclase ($\text{NaAlSi}_3\text{O}_8$); K-F: Potassium feldspar (KAlSi_3O_8); M: Muscovite ($\text{KAl}_2\text{Si}_3\text{AlO}_{10}(\text{OH})_2$); H: Hematite (Fe_2O_3); G: Goethite ($\alpha\text{-Fe}^{3+}\text{O}(\text{OH})$); L: Lepidocrocite ($\gamma\text{-Fe}^{3+}\text{O}(\text{OH})$); A: Anhydrite (CaSO_4); C: Calcite (CaCO_3); J: Jarosite ($\text{KFe}_3(\text{SO}_4)_2(\text{OH})_6$); B: Butlerite ($\text{Fe}(\text{OH})\text{SO}_4\cdot 2\text{H}_2\text{O}$); R: Rectorite ($(\text{Na,Ca})\text{Al}_4((\text{Si,Al})_8\text{O}_{20})(\text{OH})_4\cdot 2\text{H}_2\text{O}$). +++++: > 50%; ++++: 30–50%; ++: 10–30%; +: 3–10%; tr. (traces): < 3%; -: not detected.

Sample	Q	P	K-F	M	H	G	L	A	C	J	B	R
PG	++++	-	-	-	++	-	-	-	-	-	-	-
PE	++++	-	-	-	+++	-	-	-	+	+	-	-
PW	+++	-	-	++	++	-	-	-	-	-	-	+
SW	++++	-	-	-	-	+	-	+	-	-	-	-
SW-black layer	++	-	-	-	-	++++	-	-	-	-	-	-
SBB	++++	-	-	-	-	-	-	-	-	-	-	-
SB	++++	-	-	-	-	-	+	+	-	++	-	-
PGMT1	+++	++	+	-	++	-	-	++	-	-	++	-
PGMT2	++++	-	-	+	++	-	-	-	-	-	-	-
PGMT3	++++	-	-	-	+	-	-	tr.	-	-	-	-
PGMT4	++++	-	-	-	+	-	-	-	-	-	-	-

Regarding the FTIR spectra of the coloured surface samples, the following features were found (Figure 8):

- A broad band at 3340 cm^{-1} and a low intense band at 1600 cm^{-1} assigned to adsorbed water and vibration of the OH groups (O-H stretching and H-O-H bending, respectively) [33].
- Band at 2640 cm^{-1} assigned to hydrogen-bonded O-H which, with the weak band at 1400 cm^{-1} assigned to C-O stretching, suggested the presence of organic matter. These bands were negligible in PW. In the PG spectrum, organic molecules were also found

through the slight band at 2892 cm^{-1} assigned to the symmetric C-H stretching, and also a weak band at 1237 cm^{-1} corresponding to COC group vibration stretching [34]. The presence of organic matter in PG was also confirmed by bands at $800\text{--}739\text{ cm}^{-1}$ attributed to the out-of-plane bending on aromatic ring C-H bending vibrations [35].

- Bands from 1082 to 840 cm^{-1} assigned to the stretching Si-O bond of the silicon tetrahedron (around 990 cm^{-1}) and the bending vibration absorption band (at around 840 cm^{-1}).
- The doublet at 527 and 440 cm^{-1} assigned to Fe-O stretching vibrations, which is attributed to the presence of hematite [36], was detected in all the spectra.
- Moreover, in PW spectra, a band at 3600 cm^{-1} was found, attributed to O-H groups in coordination with metals [34].

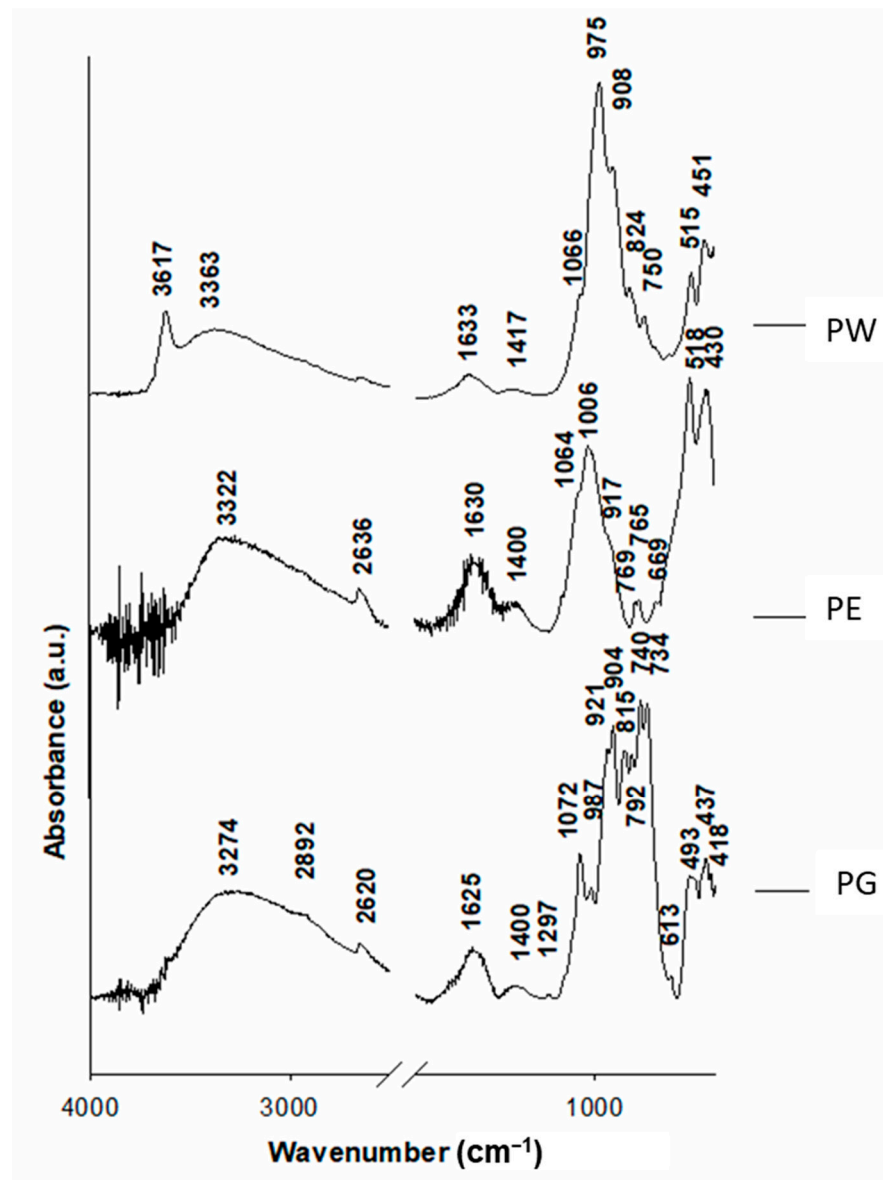


Figure 8. FTIR (absorbance) spectra of the red colorant material on the stones (PG, PW) and soil sample (PE) found in excavation.

Observations of cross-sections by stereomicroscopy and SEM allowed the characterisation of the microtexture and composition of the coloured surface samples collected in the excavation and also the red deposit–substrate boundaries of these samples (PG: Figure 9, PE: Figures 9 and 10 and PW: Figure 11). For PG, an external layer with variable thickness

was detected on the surface: from a few μm until ca. 500 μm (Figure 9A,B). This layer showed a dark red colouration (Figure 9A). SEM allowed the identification of a clean deposit–substrate boundary, suggesting that the material was deposited on the surface (Figure 9B). The substrate was rich in Si due to the quartzite substrate (Figure 9,EDS1). Moreover, it was detected a filler in fissures rich in Fe and to a lesser extent Al, Si, P, K and Ti. The layer detected on the surface was composed of a mixture of different shaped microparticles (aciculae, micrometric spheres, rhombohedral particles, etc., Figure 9C). It was rich in C, Si, Al and, to a lesser extent, Mg, Na, P, S, Cl, K, Ti and Fe (Figure 9,EDS3). Notice the remarkable difference in the intensity of the C-peak in the spectra of the external layer comparatively to that from the substrate (compare EDS1 and EDS3 in Figure 9). It is also important to note the low Fe content in the external layer, comparatively to that in the filled fissures.

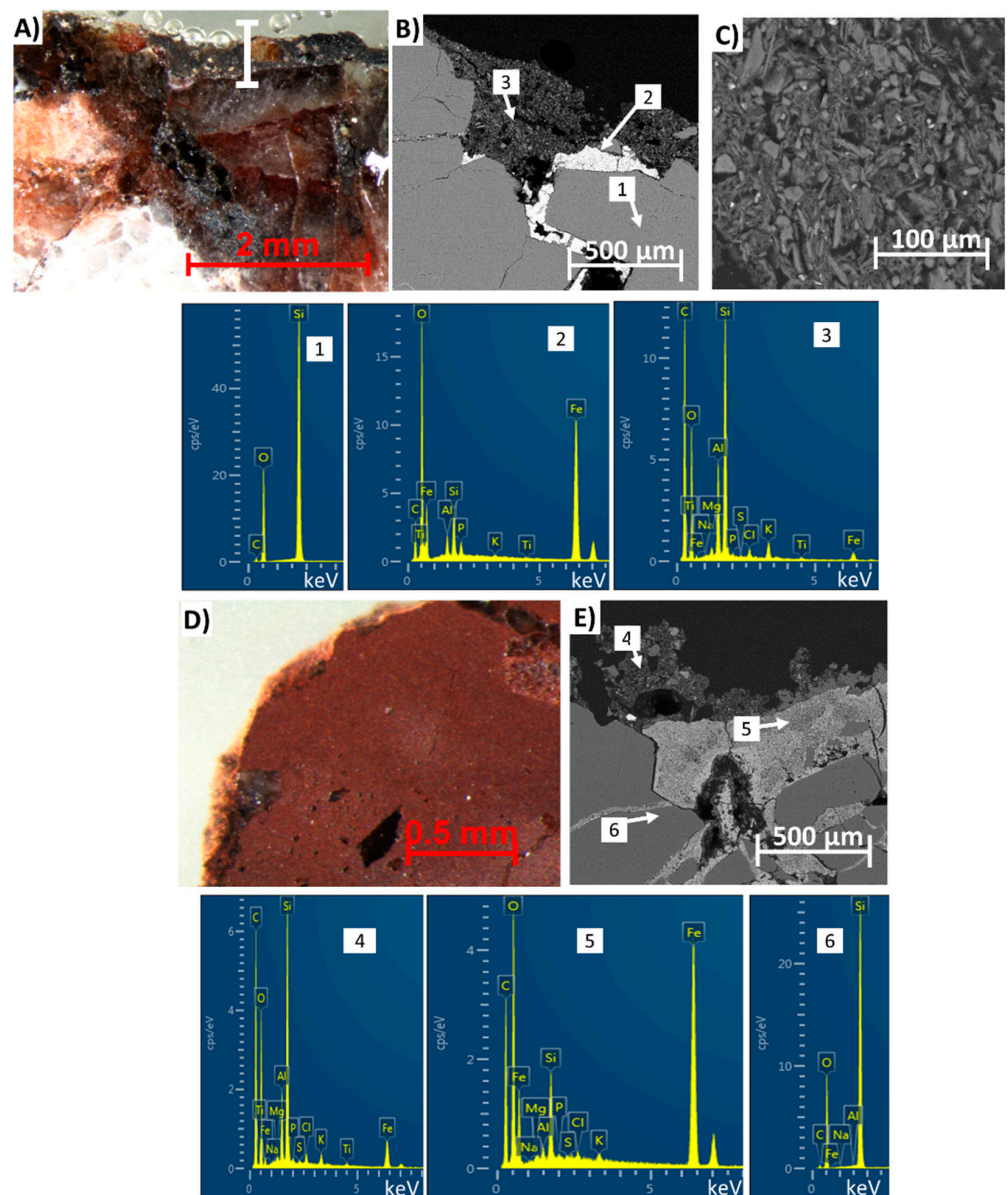


Figure 9. Micrographs of the cross-sections taken with stereomicroscopy (A,D) and SEM (B,C,E) of the red-coloured surface samples collected in the excavation: PG (A–C) and PE (D,E). Some SEM micrographs are accompanied by EDS spectra.

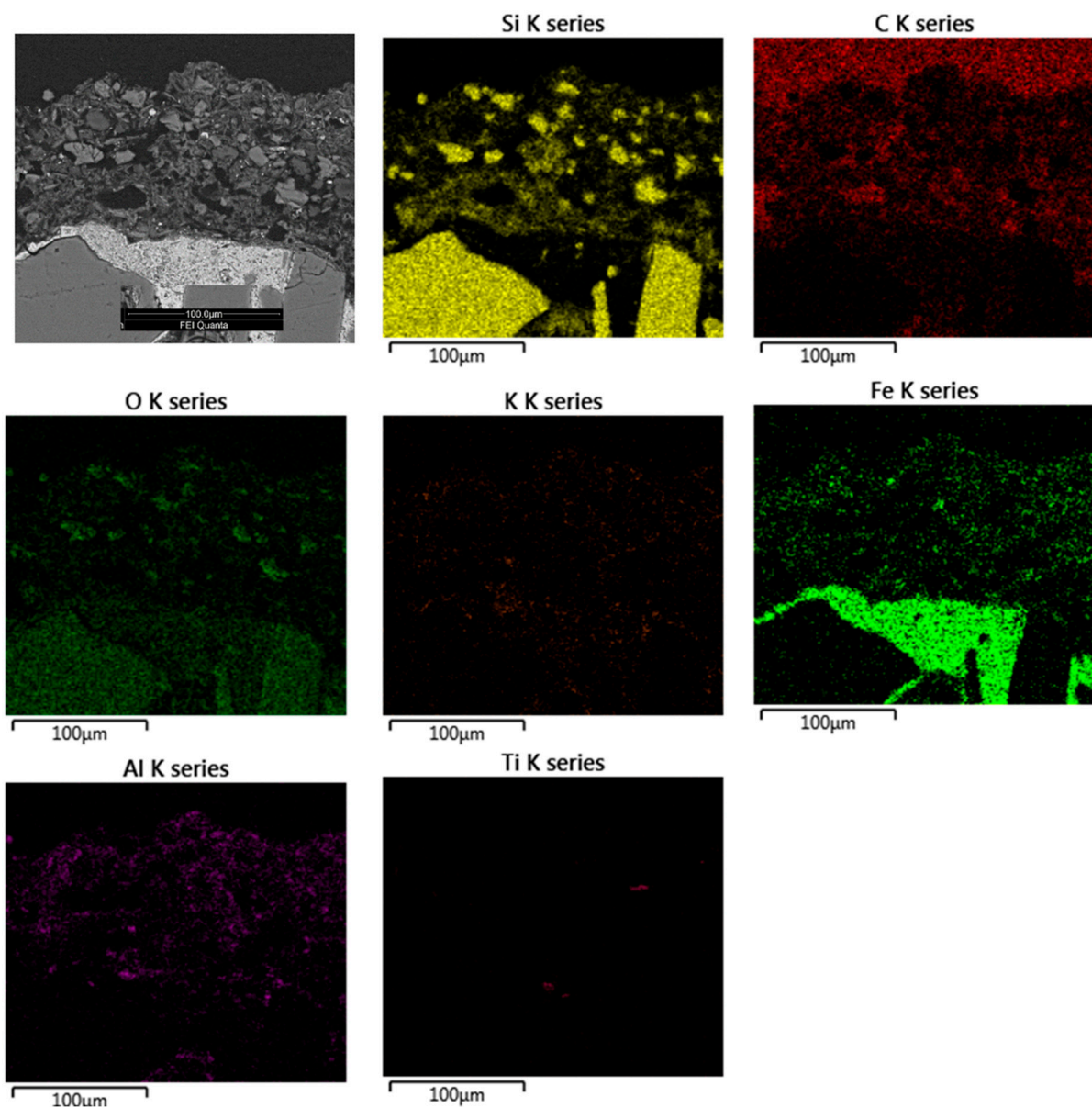


Figure 10. Compositional map of PE sample by means of SEM-EDS, showing maps of Si, C, O, K, Fe, Al and Ti.

For the PE sample, on the compact soil block, a layer with an orange colouration (Figure 9D) was detected. This external layer showed a similar thickness to that found in PG: from a few μm until 500 μm (Figure 9E). The substrate is composed of quartz (SiO_2) grains (Figure 9,EDS6) into a matrix rich in Fe and also to a lesser extent, Si, Na, Mg, Al, P, S, Cl and K (Figure 9,EDS5). The external layer seems to also be deposited on the surface, since an interaction between the external layer and the surface was not detected (Figure 9E). As was identified for PG, it is composed of C, Si and Al and to a lesser extent, Na, Mg, P, S, Cl, K, Ti and Fe (Figure 9,EDS4). As reported for PG, the external layer showed higher C content than the quartz grains underneath. Figure 10 shows the compositional map of the PE sample. The layer was composed of a mixture of micrometric particles rich in Si, Fe, K and Al. There were also isolated grains rich in Ti. The compositional map also allowed us to confirm that this layer is independent of the substrate underneath because there is a clear boundary between them.

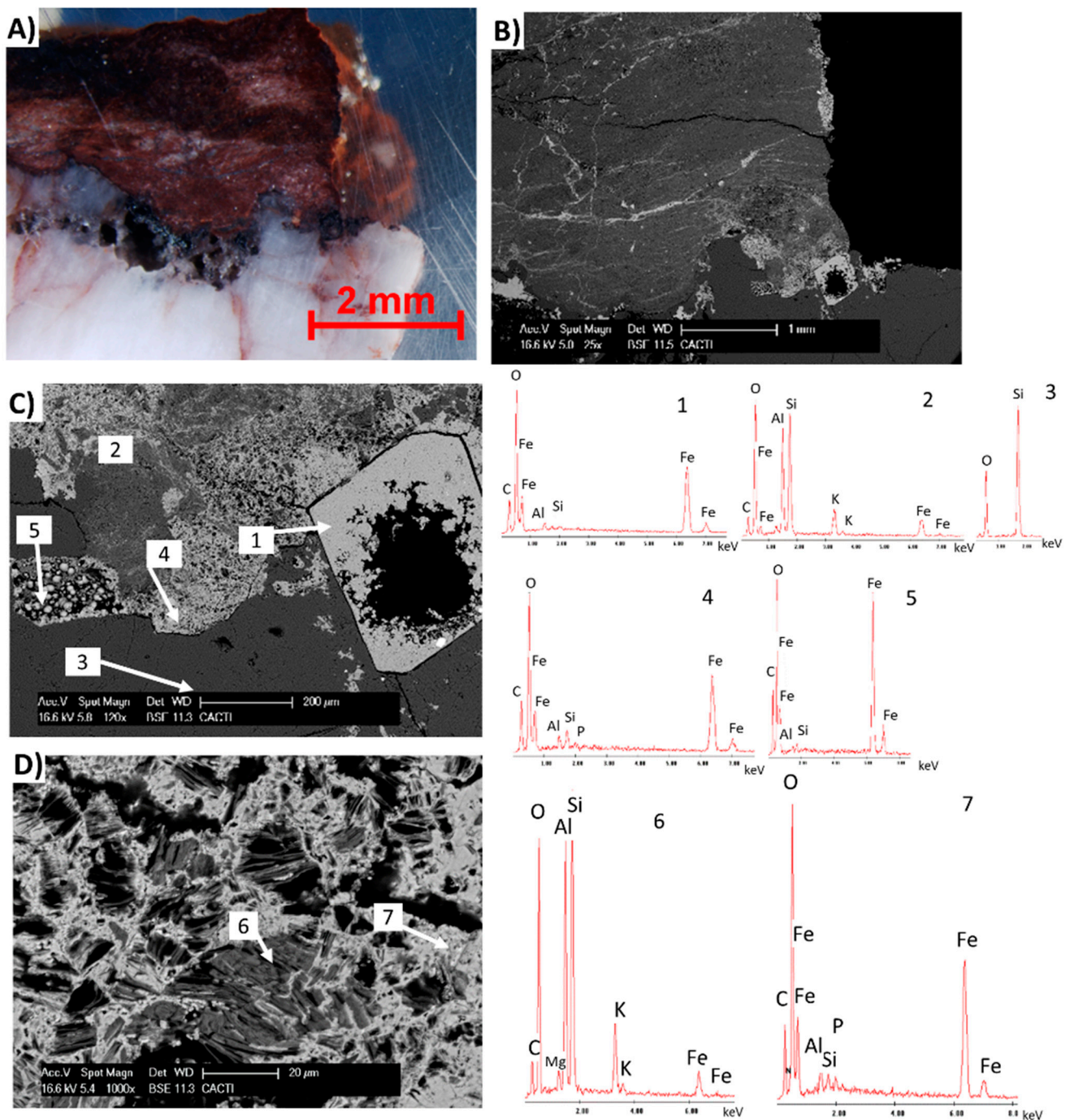


Figure 11. Micrographs of the cross-sections taken with stereomicroscopy (A) and SEM (B–D) of the PW sample collected in excavation. The SEM micrographs are accompanied by some EDS spectra.

The PW sample also revealed a red layer on the surface with a similar colour detected on the other two samples collected (Figure 11A). However, there was not a clear limit between the red layer and the quartz substrate since hematite crystals placed over the quartz grains showed signs of deterioration (Figure 11B,C). Platy crystals of hematite showed clear signs of alteration (Figure 11C). In addition, the red layer was compact, showing filled fissures with certain continuity (Figure 11B). However, the other two samples (PG and PE) did not show continuous fissures since the deposits were composed of different sized microparticles. Contrary to PG and PE, the red layer was thicker in PW (up to ca. 3 mm). Attending to the compounds of this sample, the quartz was the main component underneath the red layer (Figure 11C,EDS3). The red layer was composed mainly of Si, Al, K

and Fe (Figure 11C,EDS2). The fillers of the fissures were rich in Fe and to a lesser extent, Al, Si and P (Figure 11C,EDS4). Although these Fe-rich fillers may come from the platy hematite crystals (Figure 11C,EDS1), incipient mammillary botryoidal hematite crystals (Figure 11C,EDS5) can also contribute with Fe for the fillers. The red layer was composed of planar silicates rich in Si and Al and to a lesser extent, K and Mg (Figure 11D,EDS6), identified as muscovite by XRD. These planes were bonded by a matrix mainly rich in Fe (in minor amounts, Al, Si and P), which seemed to come from the hematite crystals (Figure 11D,EDS7). It should be noted that the C content reflected in the EDS spectra of the red layer (Figure 11C,D,EDS2,6) was similar to that detected on the quartz grains (Figure 11C,EDS3).

Figure 12 shows micrographs and EDS spectra of the three rock facies from the outcrop (SW, SBB and SB). For the SW sample, with the dark brown layer on the surface (Figure 7B), the visualisation with stereomicroscopy of the cross-section allowed a dark orange colouration below the black-brown surface layer to be identified (Figure 12A,B). SEM allowed us to identify that this orange-coloured layer with a thickness up to 200 μm was composed of quartz crystals (Figure 12B,EDS2) immersed in a Fe-rich matrix, also with Al, Si and P (Figure 12B,EDS1). In the quartz grains composing the substrate, it was possible to find cavities coated by a mineral phase rich in Fe, which may be assigned to goethite as was identified by XRD (Figure 12C,EDS3).

In the SBB sample (Figure 12D,E), it was detected a superficial layer rich in Si and to a lesser extent, Fe, Na, Al, P, S and K (Figure 12D,E,EDS4,5) belonging to the opal A speleothem. This layer was composed of two parts: the lowermost section showing a continuous and compact layer with a few μm -thickness (Figure 12E,EDS5) and the uppermost section composed of a less compact layer with more empty spaces and higher thickness: $\sim 60 \mu\text{m}$ (Figure 12E,EDS4). Moreover, opal A speleothems were also identified inside the stone (Figure 12E,EDS6).

For the SB samples which superficially showed a black colouration (Figure 7D), it was possible to identify, below this superficial black layer, an orange colouration with variable thickness, up to 50 μm (Figure 12F,G), rich in Si, S, Fe and K and to a lesser extent, Na, Al and Ti (Figure 12G,EDS8), confirming the presence of opal A speleothem with a laminar growth. Below this laminar structure, it was possible to find massive crystals rich in Fe (Figure 12G,EDS9), which can be assigned to the lepidocrocite ($\gamma\text{-FeO(OH)}$) detected by XRD. The presence of As in the lepidocrocite grains can be related to the dissolution of arsenian pyrite and subsequent mobilisation of the As^{3+} or more rarely As^{4+} [37]. In the quartz grains (Figure 12G,EDS11) of the substrate, acicular structures rich in S, Fe, K and P (Figure 12G,EDS 10) were found and assigned to the iron-hydroxysulphate mineral jarosite ($\text{KFe}_3(\text{SO}_4)_2(\text{OH})_6$) detected by XRD.

Attending to the possible colorant materials, PGMT1 (Figure 13A,B) showed the accumulation of laminar structured silicates rich in Si, Al, K and Fe as major elements and, to a lesser extent, Mg, P and Ti (Figure 13B,EDS1). Considering elemental composition by SEM-EDS and mineralogical composition by XRD, inside this laminar structure, quartz (indicated by an asterisk, Figure 13B) and hematite (indicated by an arrow, Figure 13B) grains were found.

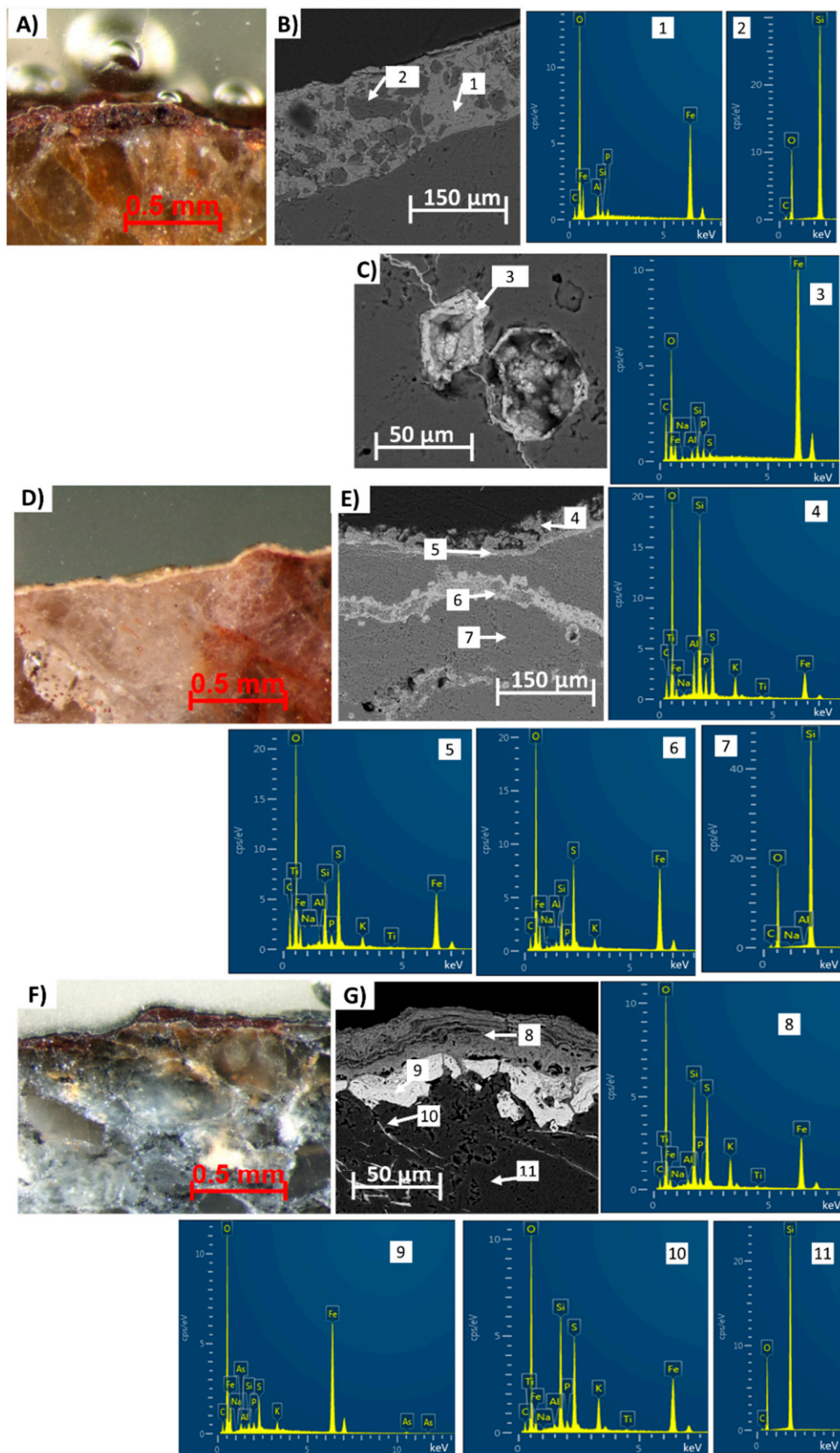


Figure 12. Micrographs of the cross-sections taken with stereomicroscopy (A,D,F) and SEM (B,C,E,G) of the stones: SW (A–C), SBB (D,E) and SB (F,G). The SEM micrographs are accompanied by some EDS spectra.

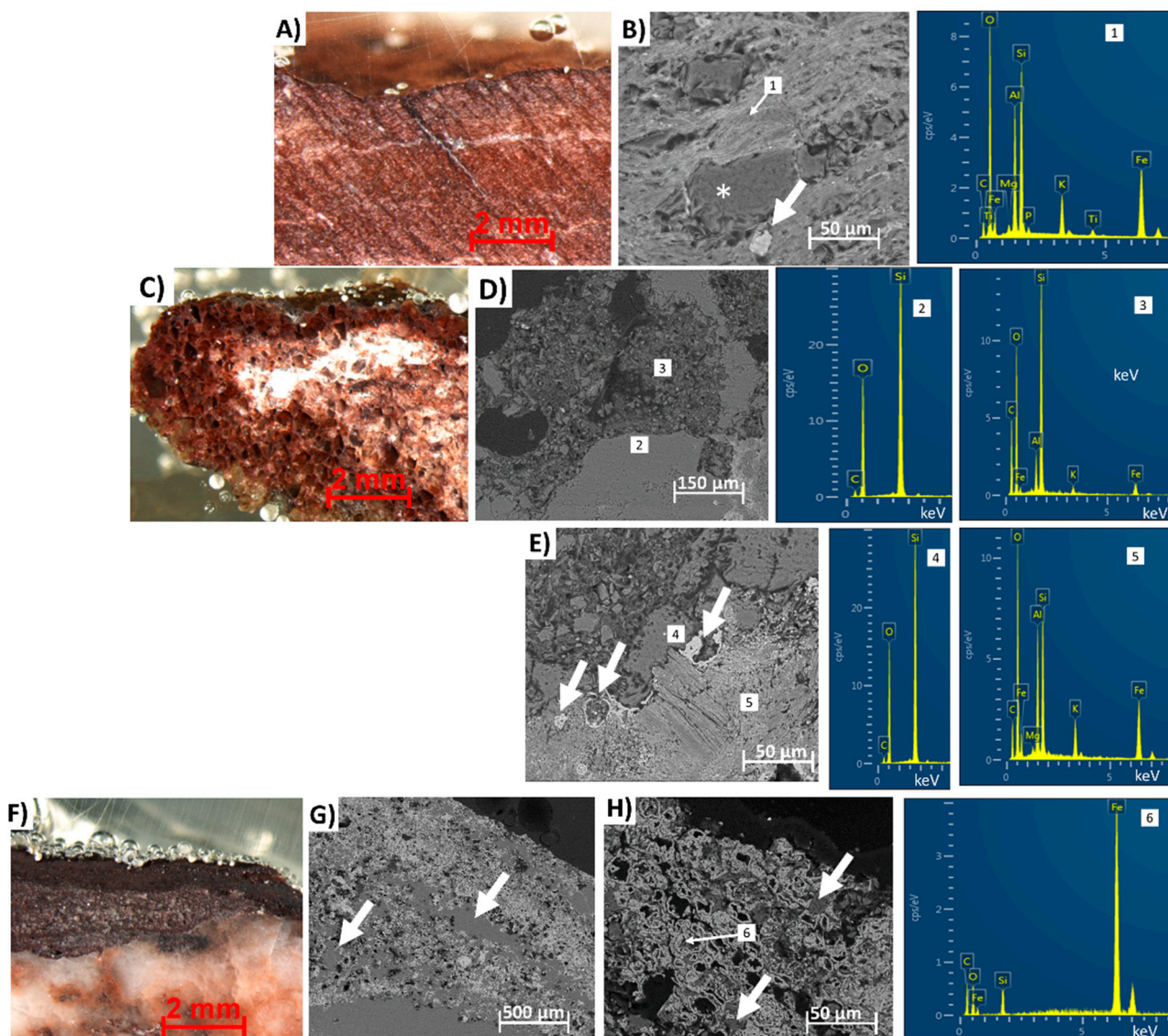


Figure 13. Micrographs of the cross-sections taken with stereomicroscopy (A,C,F) and SEM (B,D,E,G,H) of the possible colorant materials collected in the trench excavated in the northern area of Penedo Gordo: P1 (A,B), P2 (C–E) and P4 (F–H). The SEM micrographs are accompanied by some EDS spectra.

Regarding PGMT2 (Figure 13C–E), quartz grains (Figure 13D,EDS2 and 13E,EDS4), laminated silicates (Figure 13E,EDS5) showing in their composition Al, Si, Fe, K and Mg (muscovite identified by XRD) and mammillary botryoidal hematite crystals (pointed out with arrows in Figure 13E) were mixed with micrometric particles rich in Si, Fe, Al and K (Figure 13D,EDS3). The pitting found on the boundaries of the quartz grains reveals its intense weathering (Figure 13E).

Conversely to PGMT1 and PGMT2, PGMT3 and PGMT4 showed a colouration tending to purple (Figure 13F). In PGMT4, it was possible to detect a coloured layer with two different parts: the lowermost part (up to 2 mm-thick) showed a red colouration intercalated with white grains (Figure 13F) recognised as quartz grains (pointed out with arrows in Figure 13G,H), while the uppermost part (ca. 1 mm-thick) showed lower quartz content with the relative enrichment of particles rich in Fe, corresponding to botryoidal hematite grains (Figure 13G,H,EDS6).

4. Discussion

In this work, the physical and chemical characterisation of the rock paintings at Penedo Gordo, distributed across five panels, was carried out in situ using spectrophotometry and Raman spectroscopy. Additionally, red-coloured deposits (probable paint) on different substrates (grey quartzite—PG, white quartzite—PW and compact soil—PE), found in the course of the excavation of the northern trench opened below panels 3 and 4, were studied from the mineralogical, chemical and physical perspectives. Possible red colorant materials (PGMT1, 2, 3 and 4) found during excavation were also investigated as potential sources of red pigment. Moreover, three stones with the characteristic colourations found in the outcrop (white—SW, dark grey—SB and black-brownish—SBB) were also analysed.

Considering the three red-coloured surface samples, the microtexture of the red layer in the PW sample suggested that it was not a deposit of paint since it exhibited a compact deposit rich in Si, Al, K and Fe showing clear and continuous fissures filled by Fe, which may come from the hematite crystals with different habits (mammillary botryoidal and platy crystals) placed on the red layer–quartz boundary. However, in the other red-coloured samples, PE and PG, SEM allowed us to identify a mixture of microparticles rich in Si and Al and to a lesser extent, Na, Mg, P, S, Cl, K, Ti and Fe. In addition, in PW, the red layer was thicker than those detected on PG and PE: the latter samples showed layers with variable thickness from a few μm up to 500 μm , while in PW, the layer was approximately 3 mm. Moreover, it has to be considered that EDS spectra of the red layers from PG and PE showed an intense C-signal, while this signal was notably lower in the red-coloured deposit in PW. The C-content may be associated with the organic binder used to obtain the paintings. The low C content identified in PW by EDS was also confirmed by FTIR since its absorption spectra pointed to the absence or low intensity of the bands assigned to the organic matter [34,35]. Therefore, this red-coloured sample could have been considered as a source of red pigment, instead of paint. However, the presence of muscovite ($\text{KAl}_2\text{Si}_3\text{AlO}_{10}(\text{OH})_2$) and rectorite ($(\text{Na}, \text{Ca})\text{Al}_4((\text{Si}, \text{Al})_8\text{O}_{20})(\text{OH})_4 \cdot 2\text{H}_2\text{O}$), which are absent in the other two paintings (PE and PG), may suggest the contrary. Therefore, PE and PG can be considered remains of the paints used to produce the rock paintings.

In situ, spectrophotometry allowed the identification of a red colouration (increases in a^*) of the motifs accompanied with a slight decrease in the L^* comparatively to the values recorded on the natural backdrops of panels 1, 2, 4 and 5. In the motifs from panel 3, mainly a b^* increase was detected, suggesting an orange colouration which was also confirmed under the naked eye. Raman spectroscopy revealed the presence of hematite (Fe_2O_3) which is the typical red chromophore encountered in many rock art sites [6,17], as the unique red pigment in most rock paintings assigned to this period of time. Hematite was the mostly detected pigment in all motifs except some from panel 2 (Raman peaks assigned to goethite were stronger in Sp6 and Sp7 and they were weaker in Sp8 and Sp4) and in all from panel 3, where goethite was clearly detected. Additionally, for the motifs of panel 3, the presence of goethite can be the reason for the orange colouration detected by means of spectrophotometry. In the Sp 6, 7 and 8 of panel 2, the mixture of both pigments was detected by Raman spectroscopy. Therefore, colour spectrophotometry allowed the identification of the motifs produced exclusively with goethite thanks to the b^* colour parameter. These three scenarios considering the mineralogical composition detected by Raman spectroscopy ((i) hematite-based paints, (ii) goethite-based paints and (iii) hematite + goethite-based paints), could indicate that different motifs on site were produced with different raw materials, since motifs from P2 were painted with a mixture of hematite and goethite and those on P3, exclusively with goethite. This evidence suggests first that the composition of motifs on P2 may have been created in, at least, two different stages (independently of the fact that the time lapse between them cannot be established). Secondly, the representation of a human figure with a triangular-shaped head that may be assigned to the early stages of the Schematic Art tradition, typologically distinct from any other motif on site, showing a light red-orange colour, is also distinctive in terms of

pigment chemical composition. Therefore, it might be possible that the paintings on P3 belong to a particular stage (maybe the earliest) in the rock art sequence at Penedo Gordo.

It is also important to highlight that on the white stone (SW), the goethite detected was attributed to the black layer found covering the surface. A high concentration of goethite was identified in the black layer that may be assigned to the orange colouration underneath the layer. Therefore, as the possible colouring materials found in the surroundings did not show goethite, the outcrop itself could have been the source of the goethite used in some of the motifs. Hematite can be obtained from the thermal treatment of goethite at moderate temperatures (280–350 °C) [38]. However, the abundant raw materials found around the site, rich in hematite, seems to be the most plausible source to produce the paints.

In addition to the red pigments (hematite and goethite), *in situ* Raman spectroscopy also allowed the identification of silicates in the paints; analysing the coloured deposits scraped from the red surface samples in the laboratory, using XRD and FTIR, quartz was detected in all the samples (PG and PE) and in PE, calcite and jarosite were also identified. Calcite was not identified in the samples from the outcrop (SW, SB and SBB), while jarosite may also come from it because it was detected in the black-coloured stone (SB). Hence, the most plausible scenario is that pigments would have been grinded from stone fragments collected in the surrounding area. Moreover, in some of the motifs (P2: M3, P3: M2 and P4: M5), there were Raman peaks assigned to amorphous carbon [6], revealing the possible mixture of black pigments such as charcoal or soot with the red pigments. However, the absence of these peaks on other Raman spectra of the motifs on the same panel, and the existence of an amorphous carbon-rich black layer covering the surface of lower parts of the outcrop, suggest that this amorphous carbon is more likely to come from the soot that originated in fire ignitions nearby [6,13,17].

5. Conclusions

This paper details the physical, chemical and mineralogical characterisation of the motifs at Penedo Gordo (NW Spain); two panels in the northern area and three panels in the western area were documented *in situ* with different techniques of digital photographic enhancement, colour spectrophotometry and Raman spectroscopy. Having been possible to gather three red accretions on different substrates (compact soil, white quartzite and grey quartzite) during site excavation, these were subjected to laboratory analysis by means of the spectroscopic techniques XRD and FTIR, and the microscopic techniques stereomicroscopy and SEM-EDS (surface and cross-section modes). Four possible colouring materials and three stone fragments representative of the outcrop's geological features were also collected in order to study the painting–stone interaction.

It was found that hematite is the predominant pigment in the motifs. The presence of associated silicates (mainly quartz) indicates that ochres (earth pigments) were used, as opposed to pure hematite. The presence of goethite in some of the motifs on panel 2 and all the motifs from panel 3 seems to indicate the use of different sources of pigment, although other explanations for the presence of these minerals cannot be totally excluded. The chemical and mineralogical results of the possible colouring materials in the surrounding area suggest that the hematite-based pigments would have been grinded from these collected stone fragments. Moreover, black soot was detected in some of the motifs, but since the black layer, presumably from the fire, was detected on the lower parts of the outcrop, the presence of soot in the paints cannot be assigned to intentional manufacturing.

Spectrophotometry results as a suitable technique to distinguish motifs with different compositions, since the motifs from panel 3 made uniquely by goethite showed a more orange colouration than those produced with hematite. However, this analytical technique has to be used in combination with other spectroscopic analytical techniques.

From the three red accretions on different substrates, it was possible to identify that two of them were composed of a mixture of organic matter with microparticles rich in Si and Al and to a lesser extent, Na, Mg, P, S, Cl, K, Ti and Fe, which could be considered as remains of the paints used to produce the motifs on the panels above, associated with an

occupation dated to the 3rd millennium BC [2]. For the other sample, the absence of organic matter, the compact texture and the composition rich in Si, Al, K and Fe showing clear and continuous fissures filled by Fe, could be identified as raw material for rock paintings.

Author Contributions: Conceptualization, J.S.P.-A., B.C.R. and L.A.B.; Data curation, J.S.P.-A. and P.B.; Formal analysis, J.S.P.-A.; Funding acquisition, B.C.R. and L.A.B.; Investigation, J.S.P.-A., B.C.R. and L.A.B.; Methodology, J.S.P.-A., B.C.R. and L.A.B.; Project administration, B.C.R. and L.A.B.; Resources, J.S.P.-A., B.C.R., L.A.B. and P.B.; Software, J.S.P.-A., B.C.R., L.A.B. and P.B.; Supervision, J.S.P.-A. and B.C.R.; Validation, J.S.P.-A., B.C.R. and L.A.B.; Visualization, J.S.P.-A., B.C.R. and L.A.B.; Writing—original draft, J.S.P.-A., B.C.R. and L.A.B.; Writing—review & editing, J.S.P.-A., B.C.R., L.A.B. and P.B. All authors have read and agreed to the published version of the manuscript.

Funding: Project was funded by the Archeology Service—General Sub-Directorate for Conservation and Restoration of Cultural Property—General Directorate for Cultural Heritage, Ministry of Culture, Education and University Planning of the Government of Galicia, through a contract with the University of Vigo. In addition, the project had the support of the Group of Studies of Archaeology, Antiquity and Territory (GEAAT) of the University of Vigo, the Community of Mountains landholders, neighborhood of Feilas/A Trepa, and the city council of Vilardevós.

Data Availability Statement: The data presented in this study are available on request from the corresponding author.

Acknowledgments: J. Santiago Pozo-Antonio thanks the Spanish Ministry of Economy and Competitiveness (MINECO) for his “Juan de la Cierva-incorporación” (IJCI-2017-3277) post-doctoral contract. We would like to extend our thanks to Bruno Rúa, José Luis Lozano, Benito Vilas Estévez (ARBORE S.L.), David Hernández (ARBOTANTE SL) and members of the project team.

Conflicts of Interest: The authors declare no conflict of interest.

References

- Comendador, B. *Intervención Arqueológica No Penedo Gordo/Penedo da Moura. Memoria da Intervención Arqueológica 2018/2019*; Report Deposited in the General Directorate of Heritage of the Xunta de Galicia: Santiago de Compostela, Spain, 2019; Volume 2.
- Alves, L.; Comendador, B. (forthcoming). Reshaping (all kinds of) borders. The site of Penedo Gordo in the context of north-western Iberia Schematic Art. In Proceedings of the International Conference “Breaking Borders. Crossing Territories” CITCEM, Faculty of Arts and Humanities—University of Porto, Porto, Portugal, 16–18 April 2020.
- Hernanz, A.; Gavira-Vallejo, J.M.; Ruiz-López, J.F.; Edwards, H.G.M. A comprehensive micro-Raman spectroscopic study of prehistoric rock paintings from the Sierra de las Cuerdas, Cuenca, Spain. *J. Raman Spectrosc.* **2008**, *39*, 972–984. [[CrossRef](#)]
- Oliveira, C.; Bettencourt, A.M.S.; Araújo, A.; Gonçalves, L.; Kuzniarska-Biernacka, I.; Costa, L. Integrated analytical techniques for the study of colouring materials from two megalithic barrows. *Archaeometry* **2017**, *59*, 1065–1081. [[CrossRef](#)]
- López-Montalvo, E.; Roldán, C.; Badal, E.; Murcia-Mascarós, S.; Villaverde, V. Identification of plant cells in black pigments of prehistoric Spanish Levantine rock art by means of a multi-analytical approach. A new method for social identity materialization using chaîne opératoire. *PLoS ONE* **2017**, *12*, e0172225. [[CrossRef](#)]
- Rosina, P.; Collado, H.; Garcés, S.; Gomes, H.; Eftekhari, N.; Nicoli, M.; Vaccaro, C. Benquerencia (La Serena-Spain) rock art: An integrated spectroscopy analysis with FTIR and Raman. *Heliyon* **2019**, *5*, e02561. [[CrossRef](#)]
- Bikiaris, D.; Daniilia, S.; Sotiropoulou, S.; Katsimbiri, O.; Pavlidou, E.; Moutsatsou, A.P.; Chrysoulakis, Y. Ochre-differentiation through micro-Raman and micro-FTIR spectroscopies: Application on wall paintings at Meteora and Mount Athos, Greece. *Spectrochim. Acta Part A* **1999**, *56*, 3–18. [[CrossRef](#)]
- Iriarte, E.; Foyo, A.; Sánchez, M.A.; Tomillo, C. The origin and geochemical characterization of red ochres from the Tito Bustillo and Monte Castillo caves (Northern Spain). *Archaeometry* **2009**, *51*, 231–251. [[CrossRef](#)]
- Cornell, R.M.; Schwertmann, U. *The Iron Oxides: Structure, Properties, Reactions, Occurrences and Uses*; Wiley-VCH: Weinheim, Germany, 2006.
- Wainwright, I.N.M.; Helwing, K.; Rolandi, D.S.; Gradin, C.; Podestas, M.M.; Onetto, M.; Aschero, C.A. *Rock Paintings Conservation and Pigment Analysis at Cueva de las Manos and Cerro de los Indios, Santa Cruz (Patagonia), Argentina*; Preprints of the 13^o Triennial Meeting of ICOM Committee for Conservation 2: Río de Janeiro, Brazil, 2002; pp. 582–589.
- Froment, F.; Tournié, A.; Colombari, P. Raman identification of natural red to yellow pigments: Ochre and iron-containing ores. *J. Raman Spectrosc.* **2008**, *39*, 560–568. [[CrossRef](#)]
- Franquelo, M.L.; Duran, A.; Herrera, L.K.; de Haro, M.C.J.; Perez-Rodriguez, J.L. Comparison between micro-Raman and micro-FTIR spectroscopy techniques for the characterization of pigments from Southern Spain Cultural Heritage. *J. Mol. Struct.* **2009**, *924–926*, 404–412. [[CrossRef](#)]

13. Iriarte, M.; Hernanz, A.; Ruiz-López, J.F.; Martín, S. μ -Raman spectroscopy of prehistoric paintings from the Abrigo Remacha rock shelter (Villaseca, Segovia, Spain). *J. Raman Spectrosc.* **2013**, *44*, 1557–1562. [CrossRef]
14. Iriarte, M.; Hernanz, A.; Gavira-Vallejo, J.M.; Alcolea-Gonzalez, J.; de Balbín-Behrmann, R. μ -Raman spectroscopy of prehistoric paintings from the El Reno cave (Valdesotos, Guadalajara, Spain). *J. Archaeol. Sci. Rep.* **2017**, *14*, 454–460. [CrossRef]
15. Hernanz, A.; Gavira-Vallejo, J.M.; Ruiz-López, J.F.; Martín, S.; Maroto-Valiente, Á.; de Balbín-Behrmann, R.; Menéndez, M.; Alcolea-González, J.J. Spectroscopy of Palaeolithic rock paintings from the Tito Bustillo and El Buxu Caves, Asturias, Spain. *J. Raman Spectrosc.* **2012**, *43*, 1644–1650. [CrossRef]
16. Gomes, H.; Rosina, P.; Holakooei, P.; Solomon, T.; Vaccaro, C. Identification of pigments used in rock-art paintings in Gode Roriso-Ethiopia using Micro-Raman spectroscopy. *J. Archaeol. Sci.* **2013**, *40*, 4073–4082. [CrossRef]
17. Rousaki, A.; Bellelli, C.; Calatayud, M.C.; Aldazabal, V.; Custo, G.; Moens, L.; Vandennebelee, P.; Vázquez, C. Micro-Raman analysis of pigments from hunter–gatherer archaeological sites of North Patagonia (Argentina). *J. Raman Spectrosc.* **2015**, *10*. [CrossRef]
18. Venice Charter. The Venice Charter for the Conservation and Restoration of Monuments and Sites. 1964. Available online: <http://www.icomos.org/venicecharter2004/index.html> (accessed on January 2018).
19. Prinsloo, I.C.; Tounié, A.; Colomban, P.; Paris, C.; Bassett, T. In search of the optimum Raman/IR signatures of potential ingredients used in San/Bushman rock art paint. *J. Archaeol. Sci.* **2013**, *40*, 2981–2990. [CrossRef]
20. Alves, L.; Comendador, B. Arte esquemático pintado en el noroeste peninsular: Una visión integrada transfronteriza. *Gallaecia* **2017**, *36*, 11–52. [CrossRef]
21. IGME (Instituto Geológico y Minero de España). Mapa geológico de España (geological map of Spain) Serie Magna, E1:50.000. In *Hoja n° 330*, 2nd ed.; IGME: Verín, Spain, 1981.
22. CIE. S014-4/E:2007 *Colorimetry Part 4: CIE 1976 L*a*b* Color Space*; CIE Central Bureau: Vienna, Austria, 2007.
23. CR. Kimpe Clay and silt analysis. In *Soil Sampling and Methods of Analysis*. Canadian Society of Soil Science; Carter, M.R., Ed.; Lewis Publisher: Boca Raton, FL, USA, 1993; pp. 719–730, Chapter 67.
24. Burgio, L.; Clark, R.J. Library of FT-Raman spectra of pigments, minerals, pigment media and varnishes, and supplement to existing library of Raman spectra of pigments with visible excitation. *Spectrochim. Acta Part A Mol. Biomol. Spectrosc.* **2001**, *57*, 1491–1521. [CrossRef]
25. Wang, A.; Freeman, J.; Kuebler, K.E. *Raman Spectroscopic Characterization of Phyllosilicates*; Lunar and Planetary Science XXXIII; Cambridge University Press: Cambridge, UK, 2002; p. 1374.
26. Wang, A.; Valentine, R.B. *Seeking and Identifying Phyllosilicates on Mars—A Simulation Study*; Lunar and Planetary Science XXXIII; Cambridge University Press: Cambridge, UK, 2002; p. 1370.
27. Pan, A.; Rebollar, E.; Chiussi, S.; Serra, J.; González, P.; León, B. Optimisation of Raman analysis of walnut oil used as protective coating of Galician granite monuments. *J. Raman Spectrosc.* **2010**, *41*, 1449–1454. [CrossRef]
28. Coccato, A.; Jehlicka, J.; Moens, L.; Vandennebelee, P. Raman spectroscopy for the investigation of carbon-based black pigments. *J. Raman Spectrosc.* **2014**, *46*, 1003–1015. [CrossRef]
29. RRUFF Project. 2017. Available online: <http://rruff.info/> (accessed on February 2020).
30. Wray, R.A.L. A global review of solutional weathering forms on quartz sandstones. *Earth-Sci. Rev.* **1997**, *42*, 137–160. [CrossRef]
31. Romani, J.R.V.; Sánchez, J.S.; Rodríguez, M.V.; Mosquera, D.F. Speleothem development and biological activity in granite cavities. *Géomorphologie Relief Process. Environ.* **2010**, *4*, 337–346. [CrossRef]
32. Sanjurjo, J.; Romani, J.R.V.; Pallí, L.L.; Roqué, C. Opal speleothems and granite pseudocast (in Spanish). *Rev. C G* **2007**, *21*, 123–134.
33. Hwang, S.W.; Umar, A.; Dar, G.N.; Kim, S.H.; Badran, R.I. Synthesis and Characterization of Iron Oxide Nanoparticles for Phenyl Hydrazine Sensor Applications. *Sens. Lett.* **2014**, *12*, 1–5. [CrossRef]
34. Socrates, G. *Infrared and Raman Characteristic Group Frequencies: Tables and Charts*, 3rd ed.; John Wiley and Sons: Hoboken, NJ, USA, 2001.
35. Coates, G. *Interpretation of Infrared Spectra, A Practical Approach*. *Encyclopedia of Analytical Chemistry*; Meyers, R.A., Ed.; Copyright John Wiley & Sons Ltd.: Hoboken, NJ, USA, 2006. [CrossRef]
36. Salama, W.; El Aref, M.; Gaupp, R. Spectroscopic characterization of iron ores formed in different geological environments using FTIR, XPS, Mössbauer spectroscopy and thermoanalyses. *Spectrochim. Acta Part A Mol. Biomol. Spectrosc.* **2015**, *136*, 1816–1826. [CrossRef]
37. Cullen, W.R.; Reimer, K.J. Arsenic speciation in the environment. *Chem. Rev.* **1989**, *4*, 713–764. [CrossRef]
38. Gialanella, S.; Belli, R.; Dalmeri, G.; Lonardelli, I.; Mattarelli, M.; Montagna, M.; Toniutti, L. Artificial and Natural Origin of the Hematite-Based Red Pigments in Archaeological Contexts: The Case of Riparo Dalmeri (Trento, Italy). *Archaeometry* **2011**, *53*, 950–962. [CrossRef]